american physiological society
AMERICAN JOURNAL OF PHYSIOLOGY
RENAL PHYSIOLOGY

Am J Physiol Renal Physiol 327: F000–F000, 2024.
First published November 7, 2024; doi:10.1152/ajprenal.00182.2024

METHODS AND RESOURCES

Mechanisms of Tubular Transport and Adaptation to Osmotic Stress in Honor of Dr. Maurice Burg

Phosphoproteomic response to epidermal growth factor in native rat inner medullary collecting duct

AQ:1-5

AQ: au
Chung-Lin Chou, Nipun U. Jayatissa, Elena T. Kichula, Shuo-Ming Ou, Kavee Limbutara, and Mark A. Knepper

AQ: aff
Epithelial Systems Biology Laboratory, Systems Biology Center, National Heart, Lung, and Blood Institute, National Institutes of Health, Bethesda, Maryland, United States

AQ: 6

Abstract

Epidermal growth factor (EGF) has important effects in the renal collecting duct to regulate salt and water transport. To identify elements of EGF-mediated signaling in the rat renal inner medullary collecting duct (IMCD), we carried out phosphoproteomics analysis. Biochemically isolated rat IMCD suspensions were treated with 1 μM of EGF or vehicle for 30 min. We performed comprehensive quantitative phosphoproteomics using tandem mass tag (TMT)-labeling of tryptic peptides followed by protein mass spectrometry. We present a data resource reporting all detected phosphorylation sites and their changes in response to EGF. For a total of 29,881 unique phosphorylation sites, 135 sites were increased and 119 sites were decreased based on stringent statistical analysis. The data are provided to users at https://esbl.nhlbi.nih.gov/Databases/EGF-phospho/. The analysis demonstrated that EGF signals through canonical EGF pathways in the renal IMCD. Analysis of Kyoto Encyclopedia of Genes and Genomes (KEGG) pathways in which EGF-regulated phosphoproteins are over-represented in native rat IMCD cells confirmed mapping to RAF-MEK-extracellular signal-regulated kinase (ERK) signaling but also pointed to a role for EGF in the regulation of protein translation. A large number of phosphoproteins regulated by EGF contained PDZ domains that are key elements of epithelial polarity determination. We also provide a collecting duct EGF-network map as a user-accessible web resource at https://esbl.nhlbi.nih.gov/Databases/EGF-network/. Overall, the phosphoproteomic data presented provide a useful resource for experimental design and modeling of signaling in the renal collecting duct.

NEW & NOTEWORTHY EGF negatively regulates transepithelial water and salt transport across the kidney collecting duct. This study identified phosphoproteins affected by EGF stimulation in normal rat collecting ducts, providing insights into global cell signaling mechanisms. Bioinformatic analyses highlighted enhanced canonical ERK signaling alongside a diminished activity in the PI3K-Akt pathway, which is crucial for cell proliferation and survival. This EGF response differs somewhat from prior studies where both pathways were prominently activated.

growth factor; kidney; mass spectrometry; phosphorylation; protein kinase

INTRODUCTION

The kidney collecting duct plays a vital role in the maintenance of body fluid homeostasis in part by regulating transepithelial transport of salt and water. This regulation is mediated by several key hormones and autocoids including arginine vasopressin (AVP) and epidermal growth factor (EGF). EGF is produced locally in the kidney, chiefly in the thick ascending limbs of Henle's loop and the distal convoluted tubule (1). Downstream from these synthesis locations, EGF is well studied as a regulator of salt (2–6) and water transport (7–12) in the collecting duct, although the signaling pathways involved are not well studied. Although inhibition of collecting duct water transport by EGF is dependent on the presence of AVP, the inhibition of Na transporter by EGF is not. We and others have demonstrated that EGF's effect on the hydroosmotic action of vasopressin is associated with a reduction at intracellular cAMP level (11–15), which in turn, attenuated protein kinase A (PKA)-mediated phosphorylation of the aquaporin-2 water channel (AQP2) at Ser269 (12). Others have demonstrated that EGF inhibition of Na transport in collecting duct cells is mediated by classical mitogen-activated (MAP) kinases, or called extracellular signal-regulated kinases (ERK) (16–20), and may involve an increase in

AQ: 7
Correspondence: M. A. Knepper (knep@helix.nih.gov).
Submitted 21 June 2024 / Revised 25 September 2024 / Accepted 1 November 2024

J_ID: AJPRENAL ART NO: F-00182-2024 Date: 20-November-24 20:25 Page: 2 Total Pages: 21 ini: 6//EP

intracellular calcium (5). Lithium-induced nephrogenic diabetes insipidus [NDI, also known as "Arginine Vasopressin Resistance" (21)], which coincided with decreased AQP2 protein abundance, has been ascribed to changes in EGF-elicited ERK signaling (8, 22).

To have a better understanding of the complicated intracellular signaling effects elicited by EGF, it is desirable to obtain a global list of target proteins to elucidate the underlying mechanisms involved. Previously, such information has been derived from phosphoproteomics studies using quantitative mass spectrometry carried out on a variety of cancer tumor cells, from brain, breast, lung, ovarian, or immortal cervical cancer-Hela cells, which because they are in a highly proliferative state, are highly active in EGF-EGF receptor functions (23–27). Such information is however lacking in the native renal collecting duct epithelial cells that are predominately nonproliferative and differentiated.

In general, binding of EGF to the epidermal growth factor receptor (EGFR; Gene symbol: *Erbb1*) located in the basolateral plasma membrane induces receptor dimerization and increases the intrinsic tyrosine kinase activity of the receptor to self-phosphorylate tyrosine residues in its carboxyl-terminus (28, 29). Distinct phosphorylation residues on EGFR create docking sites for selective recruitment of SH2 or phosphotyrosine binding (PTB)-domain-containing adaptor proteins or signal transducers, such as GRB2, GAB1, and phospholipase Cγ, that are responsible for various functions of EGF seen in cell proliferation, survival, and differentiation (29, 30). Dimerized EGFR and ERKs are known to translocate to nuclei and exert phosphorylation effect in the nuclear proteins in addition to the cytosolic proteins (23). Nuclear proteins phosphorylated by ERK are involved in cell proliferation. Also, there is transactivation of EGFR by G-protein coupled receptors (GPCRs) (31, 32). EGF-EGFR signaling classically activates two main pathways, the mitogen-activated protein kinase (MAPK) signaling pathway and the RAC-α serine/threonine-protein kinase (AKT) signaling pathway (33–35). Hence, EGF is predicted not only to perturb tyrosine phosphorylation in target cells but also serine/threonine phosphorylation via MAPK and AKT signaling.

In the present study, to provide a resource for investigation of EGF actions in the renal collecting duct, we have carried out quantitative phosphoproteomics for global discovery of protein phosphorylation changes in isolated rat inner medullary collecting ducts (IMCDs) in response to EGF stimulation for 30 min, mimicking the time frame used in previous isolated tubule microperfusion studies (7, 12). The data are provided to users via a user-friendly set of web pages that allow searching, browsing, and downloading. We also use the data to address several questions about signaling in the collecting duct: *1*) Does EGF activate the canonical epidermal growth factor signaling pathway in native collecting duct cells? *2*) Aside from the canonical EGF-stimulated pathways, are any noncanonical pathways activated in collecting duct cells? *3*) Does EGF cause phosphorylation changes in any collecting duct water channel or solute transporter? *4*) Does EGF cause phosphorylation changes in any elements of the canonical vasopressin V2 receptor/Protein kinase A (V_2R/PKA) signaling pathway?

METHODS

IMCD Suspensions

IMCD suspensions were prepared from pathogen-free male Sprague–Dawley rats weighing 100–200 g in accordance with the NHLBI Animal Care and Use Committee Protocol Number H-0110R6. Rats were treated with furosemide (0.5 mg per rat, ip) 30 min before euthanization by decapitation to wash out the inner medullary hypertonicity and thus reduce the osmotic shock to the tissue. Rat inner medullas were dissected out, minced, and digested for 90 min at 37°C in an enzyme solution containing 3 mg/mL of collagenase B and 3 mg/mL of hyaluronidase dissolved in sucrose buffer (250 mM sucrose and 10 mM triethanolamine, pH 7.6). After digestion, the suspension was spun at low-speed centrifugations (70 *g*, 20 s, 3×) to pellet inner medullary collecting duct (IMCD) segments. The pellets were rinsed with bicarbonate buffer (118 mM NaCl, 25 mM $NaHCO_3$, 5.5 mM glucose, 5 mM KCl, 4 mM Na_2HPO_4, 2 mM $CaCl_2$, and 1.2 mM $MgSO_4$, pH 7.4 equilibrated with 5% CO_2/95% air) and finally resuspended in the same buffer solution. IMCD suspensions were incubated with EGF (1 μM) or vehicle for 30 min at 37°C in a pH- and temperature-controlled chamber (three independent pairs).

Immunoblotting

After EGF treatment, IMCDs were harvested by centrifugation (1,500 *g*, 1 min). Cell pellets were solubilized in 1× Laemmli buffer (1.5% SDS, 10 mM Tris, pH 6.8) containing 1× HALT protease/phosphatase inhibitor cocktail (Thermo Scientific), sonicated (Misonix Sonicator 3000, intensity 3, 90 s), and passed through a QIAshredder (QIAGEN, Valencia, CA). After protein concentration determination by the bicinchoninic acid (BCA) protein assay (Thermo Scientific), samples were adjusted to 2 μg/μL and 6% glycerol/40 mM DTT (DL-dithiothreitol) were added. The denatured protein samples were subjected to SDS-PAGE using 4%–20% Criterion TGX gels (BioRad, Hercules, CA). Proteins were transferred onto nitrocellulose membranes, and blocked and probed with primary antibodies overnight. Primary antibodies were anti-total EGFR (Cell Signaling, 2232S, 1:1,000) and anti-Y1091-phosphorylated EGFR (Cell Signaling, 2234S, 1:1,000) [The vendor labels their antibody as "Phospho-EGF Receptor (Tyr1068)" because of a difference in amino acid numbering convention but recognizes a site labeled as Y1091 in this paper]. The membranes were washed three times using 1× PBS with 0.1% Tween-20 followed by the application of goat anti-rabbit IRDye 680 secondary antibody (Li-Cor) for 1 h. This was followed by three additional washes and a final rinse with 1× PBS. Protein bands on the membranes were detected using the LI-COR Odyssey Scanner and analyzed with Odyssey Software v2.1.

Phosphoproteomics

After EGF treatment, IMCDs were harvested by centrifugation (1,500 *g*, 1 min). IMCDs were solubilized in 200 μL of lysis buffer containing 1% sodium deoxycholate, 1 mM sodium orthovanadate, 5 mM sodium fluoride, 1× HALT protease/phosphatase inhibitor cocktail (Thermo Scientific, Rockford, IL) in 50 mM triethylammonium bicarbonate

(TEAB) buffer, pH 7.5. Cell lysates were passed through a shredder followed by sonication (intensity 3, 90 s) and spun at 16,000 *g* for 5 min to remove insoluble components. Protein concentration in the supernatants was determined using the BCA protein assay (Pierce, Rockford, IL). One milligram of protein was used for large-scale phosphoproteome profiling (Supplemental Fig. S1).

Reduction, alkylation, and in-solution protease digestion.

Samples were reduced with 10 mM dithiothreitol in 50 mM TEAB for 1 h at 37°C and alkylated with 40 mM iodoacetamide for 1 h in the dark at room temperature. Additional 250 mM dithiothreitol was added to a final concentration of 40 mM to quench unreacted iodoacetamide. Samples were diluted to a sodium deoxycholate concentration of 0.25% and digested with trypsin/Lys-c (Promega, Madison, WI) (40 μg per 1 mg protein sample) in 50 mM TEAB (pH 7.5) overnight at 37°C.

Samples were acidified with 1% trifluoroacetic acid (TFA) to a pH of 2, vortexed, and spun at 16,000 *g* for 5 min to precipitate sodium deoxycholate. Peptide samples in the supernatant were desalted using 3-mL hydrophilic-lipophilic balance (HLB) cartridges (Waters, Milford, MA). Peptides were eluted using 70% acetonitrile/0.1% formic acid, dried in a Speedvac, and stored at −80°C. The above steps were repeated twice for a total of three replicates.

Tandem mass tag labeling.

To perform quantitative phosphoproteomics, samples from three replicates of the experiment were reconstituted in 100 μL of 100 mM TEAB and labeled using the TMT10plex Isobaric Label Reagent Set (Thermo Scientific 90110) according to the manufacturer's instruction. Samples were then combined in equal amounts in one tube. Of the sample, 1/100th was saved for total protein analysis and the remaining sample was used for phosphopeptide analysis. Samples were desalted and dried.

Phosphopeptide enrichment and high pH fractionation.

The sample used for phosphopeptide analysis was subjected to High-Select Fe-NTA kit (Thermo A32992) after reconstitution in 200 μL of binding buffer (pH adjusted to <3.5) and the flow-through was introduced into High-Select TiO_2 kit (Thermo A32993). The eluates from the two enrichments were desalted using a C18 column and dried. The Fe-NTA-enrichment and TiO_2-enrichment fractions were both resuspended in 50 μL of 10 mM TEAB, combined, and subjected to high pH reversed-phase peptide fractionation into 12 samples and dried.

LC-MS/MS analysis.

Total peptide and phosphopeptide-enriched samples were reconstituted in 0.1% formic acid. LC-MS/MS was carried out in an Orbitrap Fusion Lumos mass spectrometer (Thermo Scientific) equipped with Dionex UltiMate 3000 nano LC system and EASY-Spray ion source. Peptides were applied to a peptide nano-trap at a flow rate of 5 μL/min. The trapped peptides were fractionated with a reversed-phase EASY-Spray PepMap column (C18, 75 μm × 50 cm) using a linear gradient of 4%–32% acetonitrile in 0.1% formic acid. The time of gradient was 120 min with a flow rate of 0.3 μL/min.

Data processing and analysis.

MS spectrum raw files were searched against UniProt FASTA database "UP000002494_10116.fasta" for the rat species *Rattus norvegicus* (https://www.ebi.ac.uk/reference_proteomes/, release 2019_03_22) using MaxQuant 1.6.4.0. Specific amino acid modifications were: the tandem mass isobaric tag (tandem mass tag, TMT) of lysine (K) or N-terminus, carbamidomethylation of cysteine (C), oxidation of methionine (M), acetylation (Protein N-term), and phosphorylation of serine, threonine, and tyrosine (S, T, Y). The false discovery rate was limited to 1% using the target-decoy algorithm. Results are reported as $\log_2$ values of TMT reporter ion intensity ratios between EGF-treated samples and vehicle controls with independent control observations for each EGF-treated sample. The mass spectrometry proteomics data have been deposited to the ProteomeXchange Consortium via the PRIDE partner repository (36) (see RESULTS).

Bioinformatics.

Results were analyzed at the level of individual phosphorylation sites. TMT reporter ion intensities were $\log_2$ transformed. Predictor variables include treatment group (EGF or vehicle) and replication pair (1, 2, or 3). Dual criteria were used in the volcano plot to identify phosphosites with altered abundance, namely $|\log_2(\text{EGF/Vehicle})| > 0.3428$ and moderated P value <0.1 (Student's t test). We used the empirical Bayes' method to establish the x-axis $\log_2$(EGF/vehicle) cutoff at a 99% confidence interval for EGF versus control comparisons from the standard deviation of $\log_2$(EGF/vehicle) values across all identified phosphosites. The standard deviation of the $\log_2$(EGF/vehicle) values across all identified phosphosites is 0.1329. The 99% confidence range is calculated as [−0.3428, 0.3428], derived from 0.1329 multiplied by 2.58.

The consensus motifs for sites that were increased or decreased in abundance were analyzed by in-house Java program PTM-Logo (37). The background probabilities used for each amino acid position were assigned in a position-specific manner using frequencies downloaded from PhosphoSitePlus (https://www.phosphosite.org/). PTM Centralizer (https://esbl.nhlbi.nih.gov/PtmCentralizer/) was used to convert phosphopeptides with a single phosphorylation site to 15-amino-acid sequences with the phosphorylated amino acid in the middle.

Gene Ontology and Conserved Domain Database analysis were performed using an in-house Java application, Automated Bioinformatics Extractor (ABE, https://esbl.nhlbi.nih.gov/ABE/). To identify Gene Ontology terms that are overpresented in by using the Database for Annotation, Visualization and Integrated Discovery (DAVID, National Institute of Allergy and Infectious Diseases, v.6.7, https://david.ncifcrf.gov/). The complete IMCD transcriptome (http://dir.nhlbi.nih.gov/papers/lkem/imcdtr/) was used as the background dataset. Annotations of protein phosphorylation sites were obtained from PhosphoSitePlus (https://www.phosphosite.org/homeAction.action) or Phosphonet (http://www.phosphonet.ca/default.aspx). AQ: 11

Imaging of Intracellular Ca^{2+} in Isolated IMCD Segments

Microdissected IMCDs were transferred and immobilized on the surface of Cell-Tak-coated petri dishes and incubated with 10 μM Fluo-4/AM (Molecular Probes) in HEPES-buffered isolation fluid (in mM: 118 NaCl, 5 HEPES, 5 KCl, 2.5 Na_2HPO_4, 2 $CaCl_2$, 1.2 $MgSO_4$, 5.5 glucose, 5 Na acetate, pH 7.4 with 0.1% BSA) at room temperature for 60 min. The tubules were washed with the same solution at 37°C for another 30 min to allow de-esterification. Fluo-4 fluorescence was monitored dynamically (488-nm excitation; 525-nm emission) using a Zeiss LSM 510 confocal microscope. Fluo-4 exhibits an increase in fluorescence at 525 nm upon binding of Ca^{2+}. Images were sampled at 0.5 Hz and stored digitally. Temporal variations of Fluo-4 emission were monitored in individual IMCD cells during playback of the stored fluorescence image using MetaMorph software.

Statistics

Data are presented as means ± SE. *P* values were calculated from paired or unpaired Student's *t* test. A *P* value of less than 0.1 was considered significant for identifying significantly altered phosphosites across all three sample pairs. A *P* value of less than 0.05 was considered significant for the immunoblotting tests.

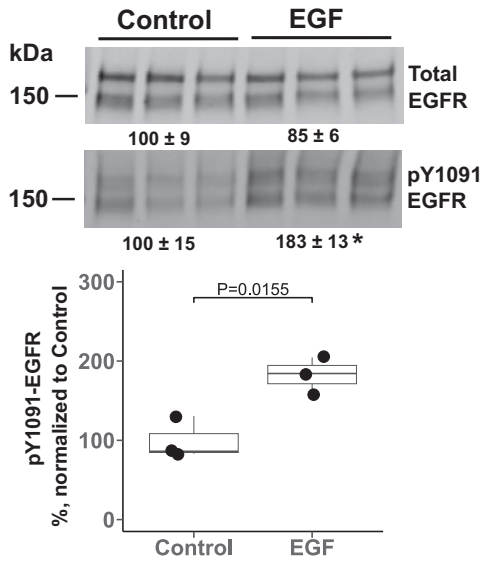

Figure 1. Immunoblot of rat IMCD suspensions using phosphospecific antibody recognizing the EGFR protein phosphorylated at Y1091, a site of autophosphorylation expected to increase with ligand-induced EGFR activation. IMCD suspensions were treated with 1 μM EGF or vehicle for 30 min. Immunoblotting was carried out using an antibody recognizing total EGFR or phospho-specific antibody recognizing pY 1091 site. Densitometry analysis was performed on both bands. The data were normalized so that the average density of the vehicle-treated samples was established as 100%. EGF significantly increased pY1091-EGFR. Values are means ± SE of band densities normalized to control. EGFR, epidermal growth factor receptor; IMCD, inner medullary collecting duct. *$P < 0.05$, unpaired Student's *t* test ($n = 3$).

RESULTS

Quantitative Phosphoproteomics: General Findings

Preliminary immunoblotting of IMCD suspensions treated with EGF (1 μM) versus vehicle showed a large increase in EGF receptor phosphorylation at an autophosphorylation site (Y1091) demonstrating that native rat IMCD cells are responsive to EGF (Fig. 1). TMT-labeling-based quantitative phosphoproteomics was carried out in rat IMCD suspensions exposed to 1 μM EGF or vehicle for 30 min ($n = 3$ each). A total of 29,881 unique phosphorylation sites were identified in EGF-treated IMCDs versus vehicle-control IMCDs. The original raw data are archived via ProteomeXchange (https://www.ebi.ac.uk/pride/login) with the data identifier PXD017192 (Username: reviewer78953@ebi.ac.uk; Password: mb0mgrmB). The full curated dataset is accessible at https://esbl.nhlbi.nih.gov/Databases/EGF-phospho/. This webpage provides user-friendly data access and is capable of being browsed, searched, or subjected to data download. In addition to the comprehensive listing on the main page, the dropdown menu presents the data sorted in different ways and filtered to isolate different subsets of the data, for example, "transcription factors," "protein kinases," "transporters," and "G-protein coupled receptors." Figure 2*A* shows a volcano plot depicting the phospho-proteomic data distribution. Specific phosphorylation sites corresponding to each point can be identified by mousing over individual points on an interactive website (https://esbl.nhlbi.nih.gov/Databases/EGF-phospho/Volcano%20plot.html) displaying all phosphoproteomic data. The proteins labeled in orange color in Fig. 2*A* are members of the Kyoto Encyclopedia of Genes and Genomes (KEGG) dataset "ERBB Pathway" (rno04012) associated with EGF signaling. Additional phosphoproteins that may play roles in the renal collecting duct are labeled in black. The dashed lines provide a set of threshold values [*P* value <0.1 and absolute value of $\log_2$(EGF/Control) > 0.3428] that demarcate the amino-acid sites most likely to have undergone a true change in phosphorylation in response to EGF (increased, 135; decreased, 119) [The threshold 0.3428 is 2.58 times the SD of all $\log_2$(EGF/Control) values, giving the 99 percent confidence interval for all quantified phosphorylation sites]. Note that of the 29,881 unique phosphorylated peptides identified, only a small fraction (0.85%) underwent changes in phosphorylation, indicative of a highly selective signaling response. Despite the fact that the EGF receptor is a tyrosine kinase, the phosphoproteomic data is dominated by serine/threonine phosphorylation indicating that other protein kinases (or phosphatases) undergo changes in activity downstream from the EGF receptor. Figure 2*B* shows changes in total protein abundances. In general, only a few proteins appeared to change in abundance, none of which correspond to the phosphopeptides that exhibited changes. Hence, phosphopeptide changes reported in Fig. 2*A* are likely due to changes in phosphorylation rather than changes in the abundance of the protein itself.

Does EGF Activate the Canonical Epidermal Growth Factor Signaling Pathway in Collecting Duct Cells?

The EGF receptor is a tyrosine kinase integral to the plasma membrane allowing activation by extracellular ligands such as EGF itself or betacellulin (12). Activation involves an increase in the intrinsic tyrosine kinase activity

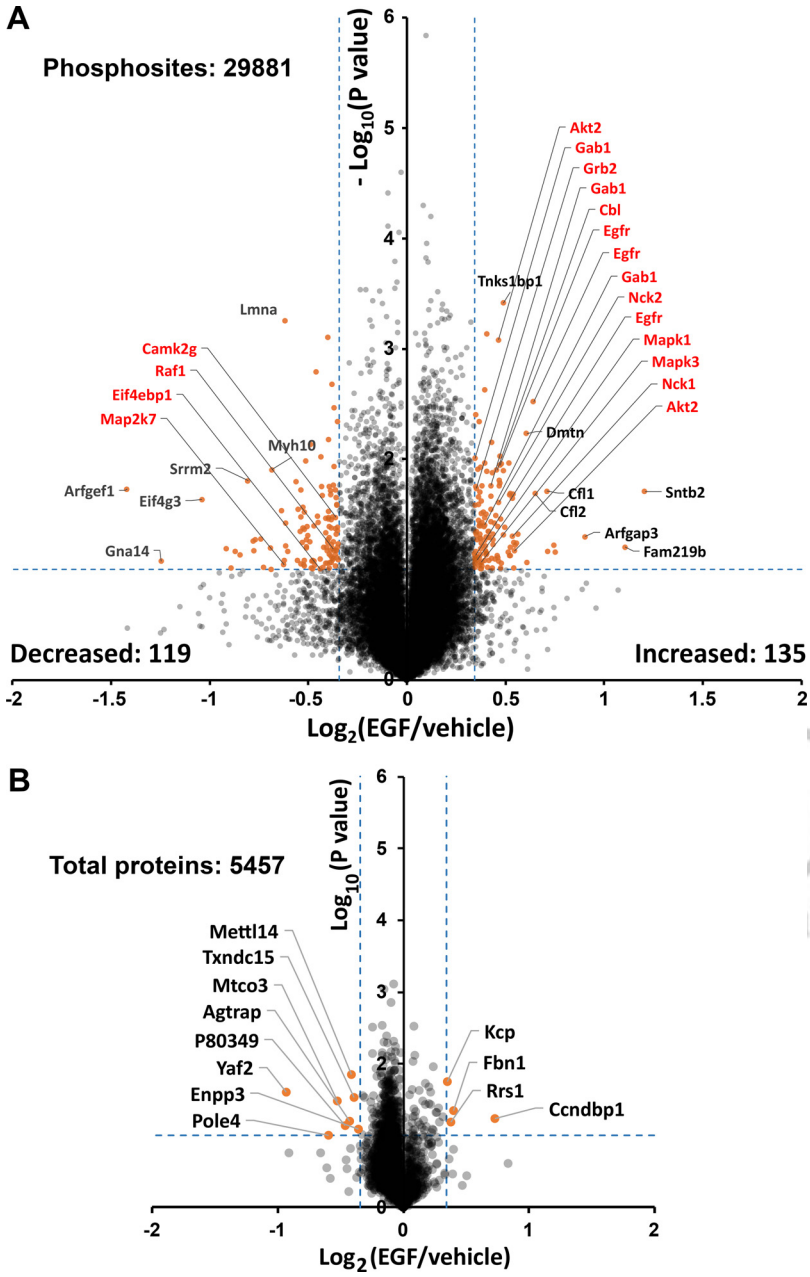

Figure 2. Volcano plot for all phosphopeptides identified from quantitative phosphoproteomics experiments (*A*) and for total protein (*B*). *A*: *x*-axis depicts $\log_2$ ratio of isobaric labeling signal of phosphosites measured in EGF-treated samples over the control samples. The *y*-axis depicts the negative of the $\log_{10}$ of *P* value determined from paired *t* tests ($n = 3$). Phosphosites that satisfied dual criteria of $P < 0.1$ and $|\log_2(\text{EGF/Control})| > 0.3428$ were used for further analysis. A $\log_2$(EGF/Control) significance cut-off level at 0.3428 was determined as the 99% confidence interval (2.58 × SD) over all phosphosites averaged over three control samples. Specific phosphophorylation sites that were significantly changed by EGF (orange dots) can be identified by hovering over individual points in online version of this graph accessible at https://esbl.nhlbi.nih.gov/Databases/EGF-phospho/Volcano%20plot.html. The proteins labeled in red font are members of the Kyoto Encyclopedia of Genes and Genomes (KEGG) dataset "ERBB Pathway "(rno04012). *B*: changes in total protein abundances in response to EGF in inner medullary collecting duct (IMCD) suspensions. Total protein levels determined from at least two peptides that map to a given protein.

COLOR

and is generally associated with the phosphorylation of tyrosine residues in the receptor. On a web page, we list all phosphopeptides with phosphorylated tyrosines (https://esbl.nhlbi.nih.gov/Databases/EGF-phospho/Phosphotyrosine.html). The rodent kidney normally expressed four EGF receptor isoforms (EGFR or ERBB1, ERBB2, ERBB3, and ERBB4) (1). Here, we found that only EGFR underwent significant phosphorylation changes in response to EGF. Increased phosphorylation at both Y1091 and Y1171 of EGFR aligns with prior documented identifying these sites as EGFR autophosphorylation sites associated with increased kinase activity (https://www.phosphosite.org/proteinAction.action?id=592&showAllSites=true) (35, 38). The specific KEGG "ERBB Pathway" phosphopeptides that changed in response to EGF are shown in Table 1. Classic growth factor receptor target sites, Y160 of GRB2 (39) as well as Y653 and Y685 of GAB1 (40), also showed significant increases in phosphorylation in response to EGF (Table 1). Overall, the observed changes in tyrosine phosphorylation confirm the efficacy of EGF in our experiments. Phosphorylation sites in Supplemental Table S1 for EGFR (Y1171), GTF2F1 (T331), SHB (Y238), TNKS1BP1 (S908), CAMK2G (T380), PEA15 (S116), and EDC3 (S159) showed changes in the opposite direction in response to the EGFR inhibitor Gefitinib in a prior phosphoproteomic study in A431 cells (41), providing further evidence for the efficacy of EGF in the present study.

In most cell types, EGF activates both the ERK pathway and the AKT pathway as documented in the KEGG ERBB pathway (https://www.genome.jp/pathway/rno04012). The data show significant increases in ERK1 (MAPK3) and ERK2

T1

J_ID: AJPRENAL ART NO: F-00182-2024 Date: 20-November-24 20:25 Page: 6 Total Pages: 21 ini: 6//EP

Table 1. *Phosphosites that change in response to EGF and are components of the KEGG "Erbb Pathway"*

Gene Symbol	UniProt ID	Site(s)	Annotation	Sequence	Log2 (Egf/Ctr)	*P*
Akt2	P47197	S461	RAC-β serine/threonine-protein kinase	YDSLGS*LELDQR	0.545	0.068
Akt2	P47197	T444;S458	RAC-β serine/threonine-protein kinase	YFDDEFT*AQSITITPPDRYDS*LGSLELDQR	0.465	0.001
Camk2g	P11730	T380	Calcium/calmodulin-dependent protein kinase type II γ	GST*ESCNTTTEDEDLKVR	−0.361	0.034
Cbl	D3ZV15	T697	Cbl proto-oncogene	LPPGEQGDSEEDT*EYMTPTSRPVGVQKPEPK	0.456	0.013
Egfr	G3V6K6	Y1091	Receptor protein-tyrosine kinase	YSSDPTSVLTEDNIDDTFLPVPEY*INQSVPK	0.643	0.003
Egfr	G3V6K6	Y1171	Receptor protein-tyrosine kinase	GSHQM@SLDNPDY*QQDFFPK	0.473	0.011
Egfr	G3V6K6	T1140	Receptor protein-tyrosine kinase	DLHYQNPHSNAVSNPEYLNT*AQPTCLSSGFDSSALWIQK	0.347	0.075
Eif4ebp1	Q62622	T69;S82	Eukaryotic translation initiation factor 4E-binding protein 1	T*PPKDLPTIPGVTS*PTSDEPPMQASQSHLHSSPEDK	−0.439	0.099
Gab1	A0A0G2JZD5	Y653	GRB2-associated-binding protein 1	GDKQVEY*LDLDLESGK	0.426	0.017
Gab1	A0A0G2JZD5	Y685	GRB2-associated-binding protein 1	NSGSGSSMSDERVDY*VVVDQQK	0.395	0.040
Gab1	A0A0G2JZD5	Y183	GRB2-associated-binding protein 1	EDPQDY*LLLINCQSK	0.347	0.010
Grb2	P62994	Y160	Growth factor receptor-bound protein 2	DIEQVPQQPTY*VQALFDFDPQEDGELGFR	0.353	0.018
Map2k7	Q4KSH7	S55	Dual specificity mitogen-activated protein kinase kinase 7	S*PSSESSPQHPTPPSRPR	−0.622	0.091
Mapk1	P63086	T179;Y185	Mitogen-activated protein kinase 1	VADPDHDHT*GFLTEY*VATR	0.354	0.083
Mapk3	P21708	T199;Y205	Mitogen-activated protein kinase 3	IADPEHDHT*GFLTEY*VATR	0.376	0.086
Nck1	A0A0G2JUA7	Y102	NCK adaptor protein 1	LY*DLNM@PAFVK	0.536	0.050
Nck2	D4A3M8	Y110	NCK adaptor protein 2	IY*DLNIPAFVK	0.468	0.025
Raf1	P11345	S295;S296	RAF proto-oncogene serine/threonine-protein kinase	SHSESASPSALSS*S*PNNLSPTGWSQPK	−0.375	0.065

KEGG Erbb Pathway: https://www.genome.jp/dbget-bin/www_bget?pathway+rno04012. EGF, epidermal growth factor; KEGG, Kyoto Encyclopedia of Genes and Genomes. *phosphorylation site; @oxidation of methionine. *P* value based on Student's *t* statistic.

(MAPK1) phosphorylation at sites associated with increased activity, MAPK3 (T199;Y205) and MAPK1 (T179;Y185), respectively (Table 1). The phosphorylation of MAPK1 (ERK2), but not MAPK3 (ERK1), at threonine and tyrosine residues within the activation loop (Thr-Glu-Tyr, TEY) was also increased in all three experiments, albeit with some variability, that is, the $\log_2$(EGF/Ctr) value for MAPK1 (T183; Y185) in three experiments: 0.389, 0.704, 0.130; *P* value: 0.133. Figure 3 shows the MS2 spectra of MAPK1 and MAPK3, and the TMT-isobaric intensity peaks identified from vehicle- and EGF-treated samples. In addition, phosphorylation of AKT2 was increased. However, the phosphorylation sites in AKT2 that increased S461 and T444/S458 (Table 1) are not the canonical sites associated with activation. Further evidence for the effects of EGF on ERK and AKT pathways was ascertained through unbiased analysis of pathways in which EGF-regulated phosphoproteins were enriched (Table 2). Overall, we conclude that EGF activates the canonical growth factor signaling pathway in native rat IMCD cells.

Aside from the Canonical EGF-Stimulated Pathways, Are Any Noncanonical Pathways Activated in Collecting Duct Cells?

Insights into noncanonical pathways regulated by EGF in native rat IMCD cells can be ascertained through gene enrichment analysis. We used the Database for Annotation, Visualization, and Integrated Discovery (DAVID) for this analysis. Several KEGG Pathway terms showed overrepresentation of EGF-regulated phosphoproteins (Table 2; Fig. 4, *top*). The enriched terms are in two groups: *1*) annotated signaling pathways including "ErbB signaling pathway," "PI3K-Akt signaling pathway," "MAPK signaling pathway," "Phospholipase D signaling pathway," "FoxO signaling pathway," and "mTOR signaling pathway"; and *2*) terms related to cell polarity, namely "Gap junction," "Tight junction," "Focal adhesion," and "Endocytosis."

Gene enrichment analysis also identified several Gene Ontology Biological Process (GO-BP) terms that showed overrepresentation of EGF-regulated phosphoproteins (Table 3; Fig. 4, *middle*). The terms "actin cytoskeleton organization" and "microtubule cytoskeleton organization" stand out, suggestive of a role for EGF in the regulation of the cell cytoskeletal structure. Three GO-BP terms are related to mRNA processing and translation, namely "mRNA catabolic process," "regulation of translation," and "nucleocytoplasmic transport."

Finally, gene enrichment analysis identified several overrepresented protein domains among the EGF-regulated phosphoproteins (Table 4; Fig. 4, *bottom*). Of particular interest is the enrichment of "PDZ domain" proteins, pointing to the roles of EGF in the formation of the tight junction and

J_ID: AJPRENAL ART NO: F-00182-2024 Date: 20-November-24 20:25 Page: 7 Total Pages: 21 ini: 6//EP

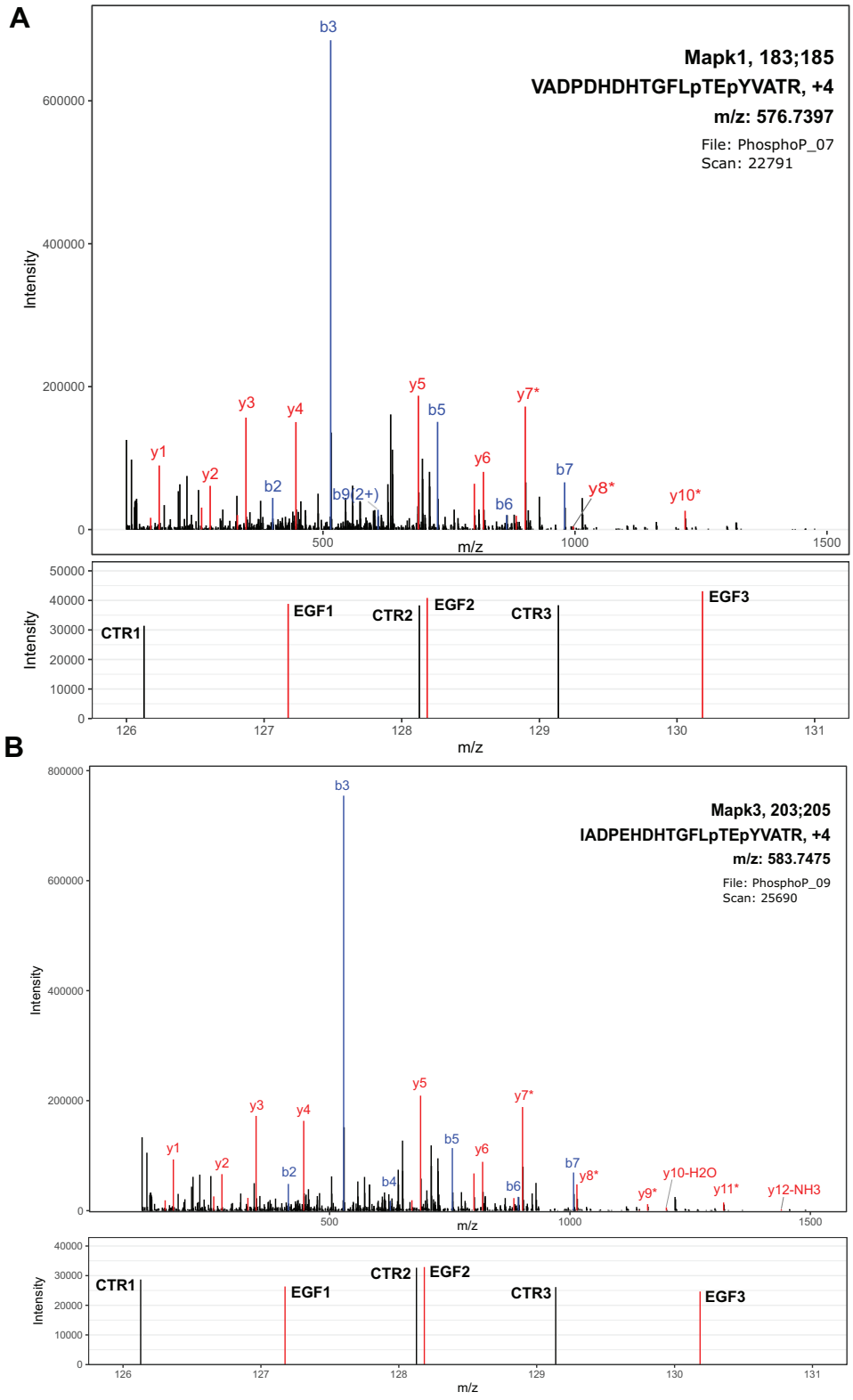

Figure 3. MS2 spectrum of EGF-induced phosphorylated ERK2 (MAPK1) and ERK1 (MAPK3) encompassing the T-E-Y activation loop. *A*: *top*: an extracted MAPK1 spectrum with phosphorylation of T183 and Y185; *bottom*: the tandem mass tag (TMT)-isobaric tag intensities from three pairs of EGF- and vehicle-treated samples. *B*, *top*: an extracted MAPK3 spectrum with phosphorylation of T202 and Y205; *bottom*: the TMT-isobaric tag intensities from three pairs of EGF- and vehicle-treated samples. CTR, vehicle-treated control samples; EGF, EGF-treated samples. AQ: 20

COLOR

cell polarity (42). The regulated phosphoproteins with PDZ domains are AHNAK, DLG3, GRIP1, PARD3B, PTPN3, SHROOM2, SHROOM3, SNTB2, TJP1, and TJP2. PDZ proteins are anchored to the plasma membrane via binding of their PDZ domains to the COOH-terminus of transporters and other integral membrane proteins and are relevant to the determination of cell polarity in epithelial cells, neurons, and other polarized cell types (43–46). Thus, EGF signaling

Table 2. *Identification of KEGG pathways whose elements are enriched in proteins with altered phosphorylation in response to EGF*

KEGG Pathway	*P* (Fisher Exact)	Fold Enrichment	Proteins
ErbB signaling pathway	0.0000008	5.48	AKT2, NCK2, EIF4EBP1, MAPK1, GRB2, MAP2K7, CBL, RAF1, CAMK2G, EGFR, MAPK3, NCK1
Phospholipase D signaling pathway	0.004	3.39	AKT2, MAPK1, GRB2, RAF1, PLPP1, EGFR, MAPK3
PI3K-Akt signaling pathway	0.004	2.46	ATF2, AKT2, SPP1, EIF4EBP1, MAPK1, GRB2, PKN1, SGK1, RAF1, EGFR, MAPK3
Gap junction	0.004	3.75	TJP1, MAPK1, GRB2, RAF1, EGFR, MAPK3
Tight junction	0.006	2.47	TJP1, EPB41L4B, PRKCI, DLG3, ARHGEF18, ARHGEF2, MAP2K7, MYH10, CGNL1, TJP2
FoxO signaling pathway	0.010	2.87	AKT2, MAPK1, GRB2, SGK1, RAF1, EGFR, MAPK3
HIF-1 signaling pathway	0.011	3.10	AKT2, EIF4EBP1, MAPK1, CAMK2G, EGFR, MAPK3
mTOR signaling pathway	0.019	2.52	AKT2, EIF4EBP1, MAPK1, GRB2, SGK1, RAF1, MAPK3
Focal adhesion	0.026	2.21	AKT2, SPP1, MAPK1, GRB2, FLNB, RAF1, EGFR, MAPK3
Endocytosis	0.032	1.85	ARFGEF1, GIT2, PRKCI, IQSEC2, MVB12A, AGAP1, ARFGAP3, CBL, PML, EGFR, RAB11FIP5
MAPK signaling pathway	0.039	1.94	ATF2, AKT2, MAPK1, GRB2, FLNB, MAP2K7, RAF1, EGFR, MAPK3

AQ:23-24 EGF, epidermal growth factor; HIF-1, hypoxia-inducible factor-1; KEGG, Kyoto Encyclopedia of Genes and Genomes.

is potentially a regulator of epithelial polarity in renal collecting duct cells through the regulation of PDZ-domain proteins.

Aiming to identify novel protein kinases downstream from the EGFR, the sites with single phosphorylated amino acids ("mono-phospho-sites") that were increased in response to EGF were used to generate a sequence preference logo using our PTM-Logo program (Fig. 5*A*). Such phosphopeptide logos represent substrate target preferences within a given pathway or by a particular protein kinase. Dominating the logo is an asparagine (N) in position +3 relative to the (S/T) phosphorylation site. Among all protein kinases profiled by Poll et al. (47) (https://esbl.nhlbi.nih.gov/Databases/Kinase_Logos/), MAP/microtubule affinity-regulating kinase 1 (MARK1) showed the most overlap with the upregulated-sites logo (Fig. 5*B*). Four MAP/microtubule affinity-regulating kinases (MARK1-MARK4) all have similar substrate preferences (47). These protein kinases are members of the SNF1 family of protein kinases that includes AMP-activated kinase and salt-inducible kinases, all with similar substrate preferences (47).

Similarly, the monophosphosites that were decreased in response to EGF gave the sequence preference logo shown in Fig. 5*C*. The aspartic acid (D) in position +2 along with the arginine (R) in position −3 points to calcium/calmodulin dependent kinase 2 (47, 48) (Fig. 5*D*). This corresponds to a set of four protein kinases (CAMK2α, CAMK2β, CAMK2γ, CAMK2δ). These kinases are well-documented components of EGF signaling (https://www.genome.jp/pathway/rno04012). However, they are not predicted to be inactivated, but rather are thought to be activated as a result of phospholipase Cγ activation and inositol (1,4,5)-trisphosphate (IP_3)-mediated calcium release. Interestingly, CAMK2γ underwent a decrease in phosphorylation at T380 (Table 1), whose effect on activity is unknown. Two other kinases were reported to have target preferences similar to CAMK2 kinases [R-X-X-(S/T)-X-D], viz., mitogen/stress-induced kinase 1 and 2, MSK1 and MSK2 (a.k.a. RPS6KA5 and RPS6KA4) (47). Finally, the strong presence of histidine (H) in position −1 among downregulated sites (Fig. 5*C*) points to the possibility of inactivation of some unknown kinase with this preference.

Looking more broadly, any of the protein kinases in Table 5 could play potential roles in EGF-dependent signaling. In addition, one protein phosphatase, PTPN3 (Tyrosine-protein phosphatase nonreceptor type) underwent altered phosphorylation in a double-phospho-peptide (S539; S546). These phosphorylation sites are unannotated with regard to the effect on function (https://www.phosphosite.org/).

Does EGF Cause Phosphorylation Changes in Any Collecting Duct Transporter(s) or Elements of the Canonical Vasopressin Signaling Pathway?

Table 6 shows transporters that underwent changes in phosphorylation. The main water channel proteins (AQP2, AQP3, and AQP4), sodium channel proteins (SCNN1A, SCNN1B, and SCNN1C), and potassium channel proteins (KCNJ1, KCNJ10, KCNJ16) all lacked evidence for altered phosphorylation in response to EGF in the current experiments. Instead, an organic anion transporter (ABCC1), an organic cation transporter (SLC22A15), a putative ammonium transporter (SLC4A11), a chloride-bicarbonate transporter (SLC4A2), and a phospholipid flippase (ATP11A) were seen to undergo phosphorylation changes. In addition, we conducted a search for proteins involved in regulating cAMP levels in collecting duct cells using a comprehensive list of proteins involved in production, degradation, and efflux of cAMP from our previous study (49). EGF caused a modest yet significant decrease in phosphorylation of the vasopressin V_2 receptor (AVPR2) at Ser255 [$\log_2$(Egf/Ctr): −0.291, *P* value: 0.049], a site that has previously been identified as vasopressin-regulated (50, 51). Reduced Na transport in response to EGF in collecting duct depends on ERK activation (16, 18, 20) and is dependent on peritubular calcium (5). To test whether EGF affects intracellular Ca^{2+}, we carried out intracellular calcium measurements in freshly isolated single IMCD tubules loaded with Fluo-4. The results show that EGF induced a small, but detectable, increase in intracellular Ca^{2+} with its magnitude lower than that induced by a protein kinase C agonist, 100 μM carbachol (Fig. 6). This result is in agreement with Ca^{2+} measurements in rat IMCD done previously using a different Ca^{2+} indicator dye, Fura-2 (52).

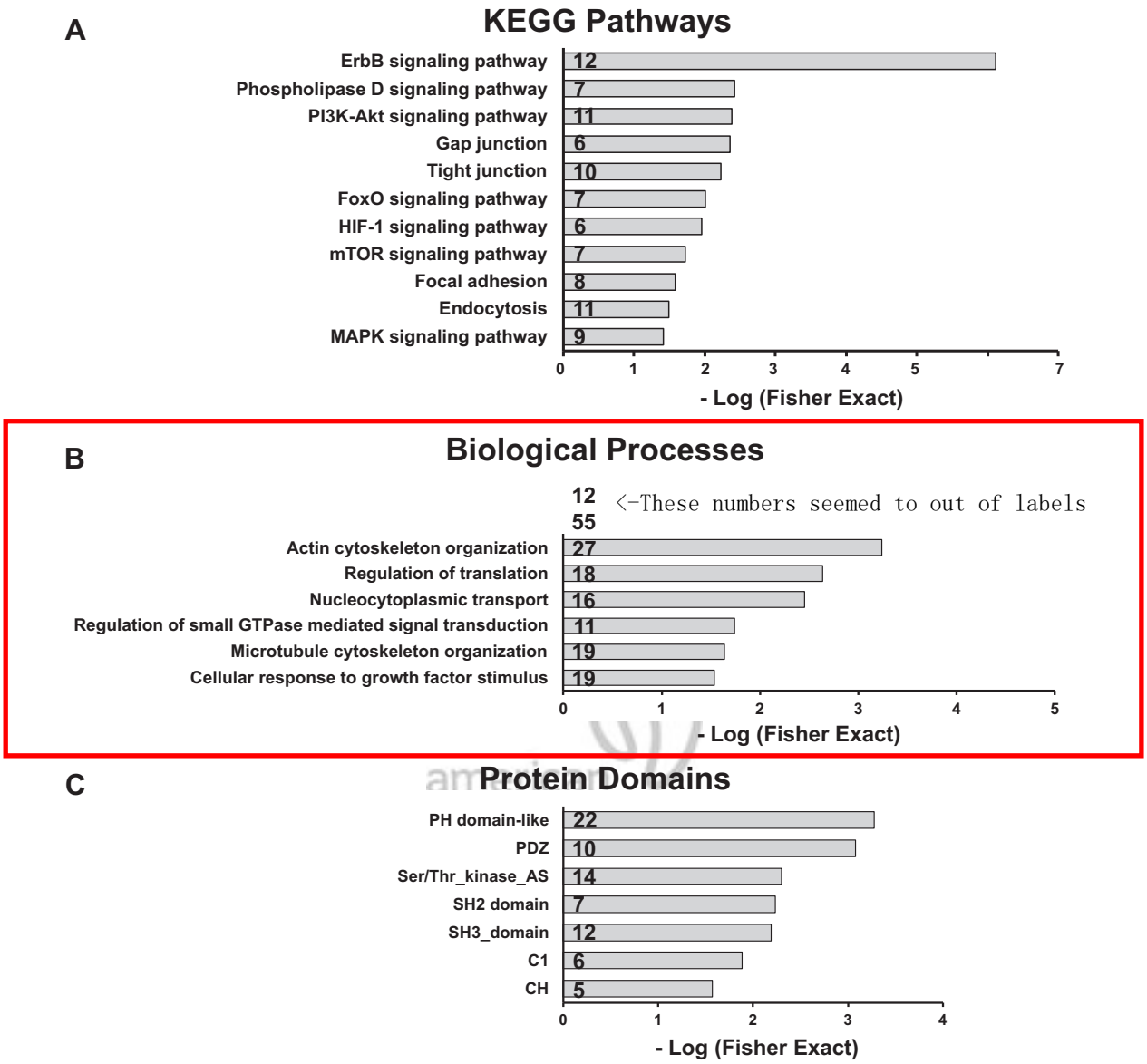

Figure 4. Bioinformatic analysis of EGF-regulated phosphoproteins using the Database for Annotation, Visualization and Integrated Discovery (DAVID). Classifiers identified significant overrepresentation of regulated phospho-proteins in KEGG Pathways (*A*). *B*: Gene Ontology Biological Processes. *C*: Protein Domains. The official gene symbols of EGF-regulated phosphoproteins were uploaded to DAVID website using all identified phosphoproteins as background for functional annotation clustering. Bar heights show significance level calculated as $-\log_{10}(P)$ for Fisher Exact tests. The integers within the bar indicate the number of phosphoproteins that match each classifier. EGF, epidermal growth factor; KEGG, Kyoto Encyclopedia of Genes and Genomes.

Functional Classification of EGF-Dependent Phosphorylation Sites in Collecting Duct

To offer an overview of the comprehensive effects of EGF in rat IMCD, we mapped the phosphorylation sites altered by EGF to functional classifiers in Fig. 7. This figure has been posted as a user-accessible webpage at https://esbl.nhlbi.nih.gov/Databases/EGF-network/. Users can find functional classifiers of interest and identify phosphoproteins that can be studied further. We have also constructed a causal map showing pathways hypothetically involved in EGF signaling in the collecting duct (Fig. 8), which comprises nodes for the regulated phosphoproteins and edges for the direction of effects based on literature searching and data from this study (summarized in Table 7).

Database Comparison: EGF versus dDAVP

Figure 9 compares the present dataset with a dDAVP-induced phosphoproteome generated in our laboratory using the same methodologies (53). Of a total of 5,655 unique phosphorylation sites matched in both datasets, 231 were significantly changed by either EGF or dDAVP and only four were found significantly changed by both EGF and dDAVP. Of these four, only the FERM protein EPB41l4B at S401, an upstream regulator of Rho guanine nucleotide exchange factor 18 (ARHGEF18) that plays a role in actin cytoskeleton reorganization, was found to have opposite changes in response to EGF and dDAVP. Also, both KAZN (S357) and LIMD1 (S233) were significantly decreased and POC5 (S80) was significantly increased in both EGF and dDAVP studies.

Table 3. *Identification of GO-biological processes enriched in proteins with altered phosphorylation in response to EGF*

Gene Ontology-Biological Process Term	*P* (Fisher Exact)	Fold Enrichment	Proteins
mRNA catabolic process	0.00007	3.71	UPF2, TNRC6C, PTBP1, ZHX2, THRAP3, CNOT2, AGO1, HNRNPD, CASC3, YBX1, GTPBP1, EDC3
Cell development	0.0005	1.51	ZMYND8, JADE2, SHB, LIMD1, AKAP13, GRIP1, PTBP1, POF1B, AKT2, CFL2, PALM, CFL1, NCK2, KIF1A, NCK1, MED1, PRKCI, ZHX2, MAP1S, SHROOM3, MSH2, PEAK1, MAP1B, ARHGEF2, SGK1, RAF1, PLEC, ANP32A, MYCBP2, EGFR, RAP1GAP, RNF2, CUX1, CLMN, MAP2, LMNA, SPP1, MAP7, MAPK1, FLNB, MAP4, DISC1, CAMK2G, MYH10, MAPK3, ARFGEF1, DMTN, USP9X, FOSL2, TJP1, ABI1, GRB2, EIF4G3, FBN1, TJP2
Actin cytoskeleton organization	0.001	1.93	ARHGAP6, AKAP13, EPB41L4B, POF1B, CFL2, EPB41L2, CFL1, NCK2, FLNB, MYH10, CGNL1, NCK1, ARFGEF1, PRKCI, DMTN, IQSEC2, CAVIN3, SHROOM2, ARHGEF18, SHROOM3, CDC42BPB, SPTB, TJP1, SPECC1L, GRB2, ARHGEF2, PLEC
Regulation of translation	0.002	2.08	CASC3, YBX1, LIMD1, EEF2, PML, TNRC6C, PTBP1, ALKBH5, THRAP3, AKT2, AGO1, NCK2, HNRNPD, EIF4EBP1, MAPK1, EIF4G3, MAPK3, NCK1
Nucleocytoplasmic transport	0.004	2.10	RANBP2, MED1, ATF2, RANBP3, ANP32A, NUP133, NUP153, SUPT6H, PML, AKAP13, ALKBH5, RSRC1, LMNA, CFL1, HNRNPD, MAPK1
Regulation of small GTPase-mediated signal transduction	0.018	2.04	ITPKB, ARFGEF1, AKAP13, GIT2, IQSEC2, DENND4C, ARHGEF2, CBL, ARFGEF3, CGNL1, RAP1GAP
Microtubule cytoskeleton organization	0.023	1.62	MAP1S, PEX14, PARD3B, STAG1, MAP2, MAP1B, CCDC8, SPECC1L, LMNA, CFL1, MAP7, FLNA, TACC2, MAP4, ARHGEF2, DISC1, SGK1, MARK3, MDM1
Cellular response to growth factor stimulus	0.029	1.59	MED1, ATF2, USP9X, LEMD3, EEF2, CBL, PML, RAP1GAP, EGFR, TNRC6C, GRIP1, MAP1B, CFL1, GRB2, RAF1, MAPK3, BPTF, BCL9L, FBN1

EGF, epidermal growth factor; GO, gene ontology.

These results suggest a high degree of independence between EGF signaling and vasopressin signaling in collecting duct cells.

DISCUSSION

In this paper, we present a comprehensive phosphoproteome of native IMCD cells in response to 30 min of EGF stimulation. Our goal is to identify proteins and signaling pathways linked to EGF's effect on osmotic water permeability, as previously reported (7, 12). This dataset provides a resource that can be used to design and interpret future studies. The resource included a user-friendly web page where the data can be downloaded, browsed, or searched, along with several ancillary pages that highlight different subsets of phosphoproteins. This phosphoproteomic dataset, however, has two notable limitations. First, it lacks a time-dependent element of EGF response, which has been demonstrated previously in time-course experiments conducted in nonomics studies (12, 54) or phosphoproteomics studies (24, 25). These studies have shown that ERK and its upstream kinases exhibit time-dependent phosphorylation changes. The lack of this temporal aspect may account for the absence of several EGF-activated proteins encoded by immediate early response genes (IEGs), such as c-Fos, C-Jun, Egr-1, c-Myc and Fosl1, or by delayed early genes (DEGs) in our study (55). Second, our study used a relatively high EGF concentration. Breyer et al. reported that EGF at 0.01 μM reduced vasopressin-stimulated osmotic water permeability in rabbit cortical collecting ducts (CCDs) by 50%, whereas our recent study found that EGF at 0.1 μM inhibited osmotic water permeability in rat IMCDs by only 27% (12). This discrepancy in EGF responsiveness may stem from species differences or the specific collecting duct segments examined. AQ: 14

Table 4. *Identification of protein domains enriched in proteins with altered phosphorylation in response to EGF*

Domain	*P* (Fisher Exact)	Fold Enrichment	Proteins
PH domain-like	0.0005	2.11	RANBP2, RABGAP1, RANBP3, IQSEC2, LRBA, ARHGEF18, AGAP1, CDC42BPB, ARHGAP27, SPTB, PLEKHA7, AKAP13, TBC1D1, EPB41L4B, AKT2, EPB41L2, ARHGEF2, KIF1A, ARHGEF40, TNS1, SNTB2, PTPN3
PDZ	0.0008	3.26	TJP1, GRIP1, DLG3, AHNAK, SHROOM2, SHROOM3, SNTB2, TJP2, PTPN3, PARD3B
Ser/Thr_kinase_AS	0.005	2.16	NEK9, PRKCI, PRPF4B, CDC42BPB, SRPK1, AKT2, MAPK1, PKN1, MAP2K7, SGK1, RAF1, CAMK2G, MARK3, MAPK3
SH2 domain	0.006	3.17	NCK2, GRB2, SHB, CBL, SUPT6H, TNS1, NCK1
SH3_domain	0.007	2.25	TJP1, DLG3, FNBP1, ABI1, NCK2, GRB2, ARHGAP27, FNBP1L, SH3D19, TJP2, PLEC, NCK1
C1	0.013	3.03	AKAP13, PRKCI, CDC42BPB, ARHGEF2, RAF1, TNS1
CH	0.027	2.91	CLMN, SPECC1L, FLNB, SPTB, PLEC

EGF, epidermal growth factor.

J_ID: AJPRENAL ART NO: F-00182-2024 Date: 20-November-24 20:25 Page: 11 Total Pages: 21 ini: 6//EP

COLOR

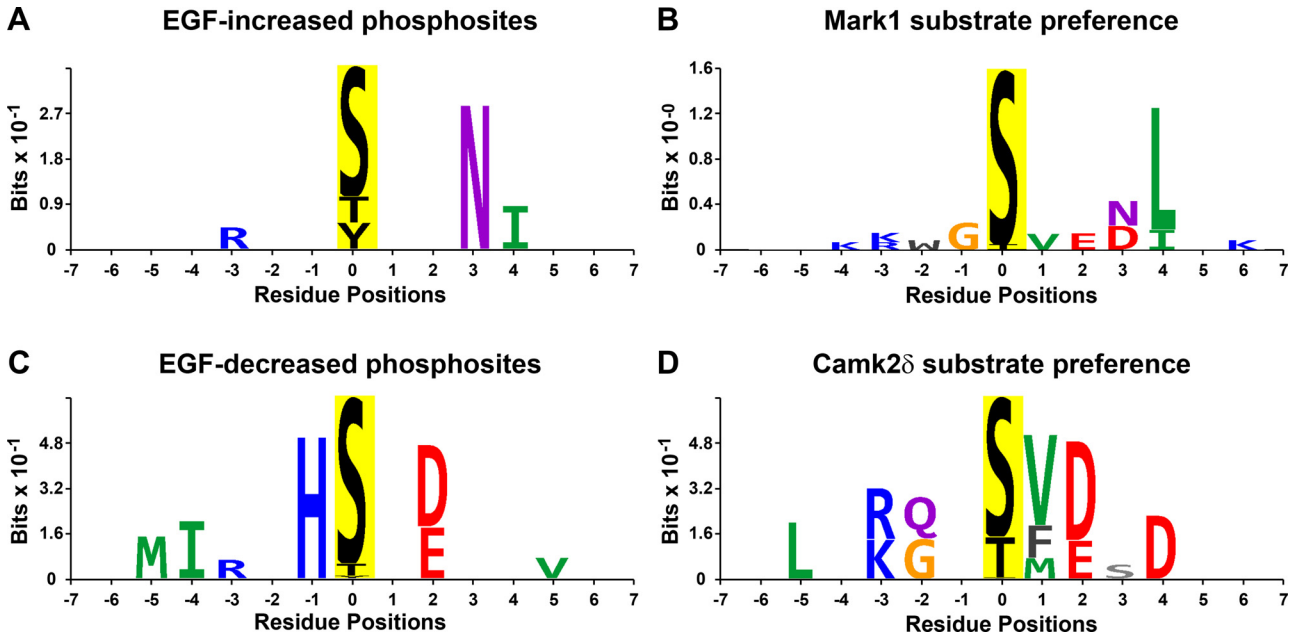

Figure 5. Phosphopeptide motif analysis using in-house Java application PTM-Logo. *A*: mono-phosphosites upregulated in response to EGF were used to create a sequence preference motif using all monophosphosites as background. *B*: MARK1 substrate preference logo generated from Poll et al. (47). The sequence from *A* was input into KinasePredictor (https://esbl.nhlbi.nih.gov/Databases/Kinase_Logos/KinasePredictor.html) to identify kinases most likely responsible and the resulting motif was downloaded from https://esbl.nhlbi.nih.gov/Databases/Kinase_Logos/. *C*: mono-phosphosites downregulated in response to EGF were used to create a sequence preference motif using all monophosphosites as background. *D*: Camk2δ substrate preference logo generated from Poll et al. (47). EGF, epidermal growth factor.

Supporting evidence suggests a higher EGF binding affinity in CCDs compared with IMCDs (56), and greater EGF immunoreactivity in intercalated cells than in principal cells in the human collecting duct (57). Given that we previously observed reliable inhibition of vasopressin-elicited PKA activation at 1 μM EGF (12), we opted for this higher concentration to enhance the identification of phosphorylation changes in the present study. The large-scale phosphoproteomics data

AQ: 25

Table 5. *Phosphosites corresponding to protein kinases with altered abundance in response to EGF in native rat IMCD cells*

Kinases	UniProt ID	Site	Annotation	Kinase Family	Direction of Change	Effect on Activity
Akt2	P47197	S461	RAC-β serine/threonine-protein kinase	AGC	Up	NA
Akt2	P47197	T444;S458	RAC-β serine/threonine-protein kinase	AGC	Up	NA
Camk2g	P11730	T380	Calcium/calmodulin-dependent protein kinase type II subunit γ	CAMK	Down	NA
Cdc42bpb	Q7TT49	S1685;S1692	Serine/threonine-protein kinase MRCK β	AGC	Down	NA
Cdc42bpb	Q7TT49	S1685;S1695	Serine/threonine-protein kinase MRCK β	AGC	Down	NA
Cdc42bpb	Q7TT49	S1688;S1695	Serine/threonine-protein kinase MRCK β	AGC	Down	NA
Egfr	G3V6K6	T1140	Receptor protein-tyrosine kinase	Tyr	Up	NA
Egfr	G3V6K6	Y1091	Receptor protein-tyrosine kinase	Tyr	Up	Increase
Egfr	G3V6K6	Y1171	Receptor protein-tyrosine kinase	Tyr	Up	Increase
Map2k7	Q4KSH7	S55	Dual specificity mitogen-activated protein kinase kinase 7	STE	Down	NA
Mapk1	P63086	T179;Y185	Mitogen-activated protein kinase 1	CMGC	Up	Increase
Mapk3	P21708	T199;Y205	Mitogen-activated protein kinase 3	CMGC	Up	Increase
Mark3	Q8VHF0	S396	MAP/microtubule affinity-regulating kinase 3	CAMK	Down	NA
Nek9	A0A0G2K8N9	S20	NIMA-related kinase 9	NEK	Down	NA
Nek9	A0A0G2K8N9	S330;T334	NIMA-related kinase 9	NEK	Up	NA
Peak1	D4A563	S823	Pseudopodium-enriched atypical kinase 1	Other	Down	NA
Pkn1	Q63433	S582;S607	Serine/threonine-protein kinase N1	AGC	Down	NA
Prkci	F1M7Y5	T13	Protein kinase C iota type	AGC	Down	NA
Prpf4b	Q5RKH1	S518;S519;S520	Serine/threonine-protein kinase PRP4 homolog	CMGC	Up	NA
Raf1	P11345	S295;S296	RAF proto-oncogene serine/threonine-protein kinase	TKL	Down	Increase
Sgk1	Q06226	S395;S396;S400	Serine/threonine-protein kinase Sgk1	AGC	Up	NA
Srpk1	A0A0U1RRU0	T453	SRSF protein kinase 1	CMGC	Down	NA

EGF, epidermal growth factor; IMCD, renal inner medullary collecting duct.

Table 6. *Transporters with altered phosphorylation in response to EGF*

Gene Symbol	UniProt ID	Site(s)	Function	Sequence	Log2 (Egf/Ctr)	*P*
Abcc1	Q8CG09	S919;S930	Organic anion export	HLSNSS*SHSVVTNQQHS*STAELQK	−0.395	0.035
Atp11a	D4A7K5	S450	Phospholipid flippase	ECCIEGHVYVPHVICNGQVLPDS*SGIDMI-DSSPGVSGR	0.370	0.048
Slc22a15	D4A271	S525;S528;S530	Organic cation transporter	ASS*LGS*ES*EEEEEEFYDANEETQMIK	0.431	0.080
Slc4a11	D3ZVP9	S47;S48;S54	Putative ammonium transport	EDSLGDEVFDTVNS*S*IVSGES*IR	0.346	0.079
Slc4a2	P23347	S145;S148;S149	Chloride-bicarbonate exchanger	APPQQPS*PAS*S*PSAVQFFLQEDEGTDR	0.376	0.012

EGF, epidermal growth factor. *phosphorylation site. *P* value based on *t* statistic.

presented in this paper provides a starting point for future studies to investigate their physiological significance using genetic manipulation. One such example of this is the recent identification of Camk2d target proteins, achieved through a combination of CRISPR-Cas9 gene deletion technique and phosphoproteomics (48).

The general picture arising from the bioinformatic analysis is that EGF stimulation leads to phosphorylation changes in several key components of the canonical MAP kinase signaling pathway, specifically the RAF-MEK-ERK cascade. Autophosphorylation of EGFR on Y1171 facilitates RAS activation and subsequent ERK phosphorylation. The effects on

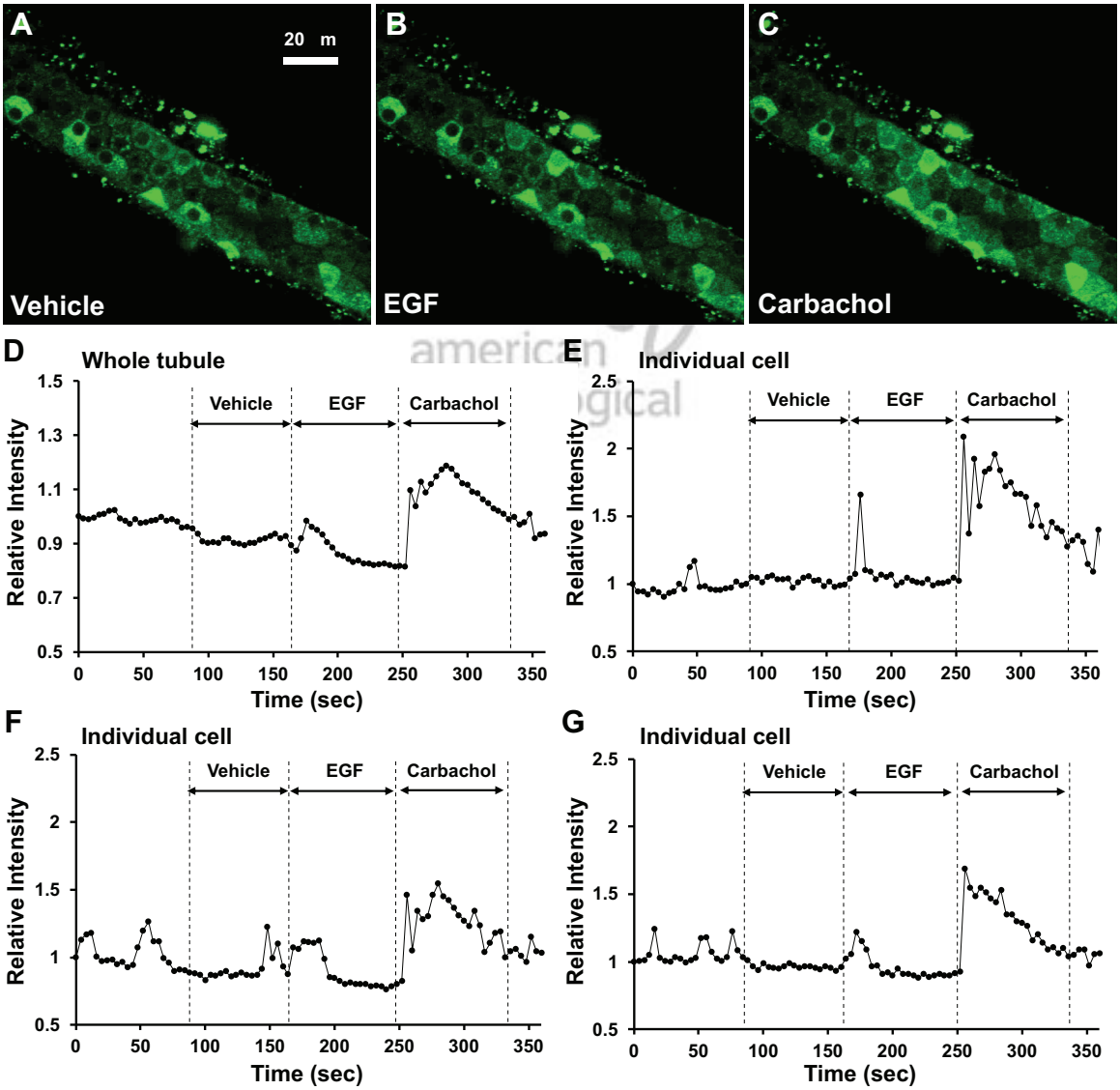

Figure 6. Effect of EGF on intracellular Ca^{2+} of rat IMCD measured by Fluo-4 fluorescence. Freshly isolated rat IMCD segments were microdissected and loaded with calcium indicator dye, Fluo-4. The same tubule was treated in order with vehicle, 0.1 μM EGF, and 100 μM carbachol with a brief wash in between treatments ($n = 3$). *A–C*: representative fluorescence images in response to vehicle, EGF, and carbachol stimulation. *D*: plotting of fluorescence intensity as a function of time acquired at the tubule level. *E–G*: plotting of fluorescence intensity as a function of time acquired at the single-cell level. Injection of vehicle did not alter Ca signal, whereas injection of 0.1 μM EGF induced a small, transient, increase in intracellular Ca^{2+} that was lower in magnitude than that induced by 100 μM carbachol (see Supplemental Video S1).EGF, epidermal growth factor; IMCD, inner medullary collecting duct.

COLOR

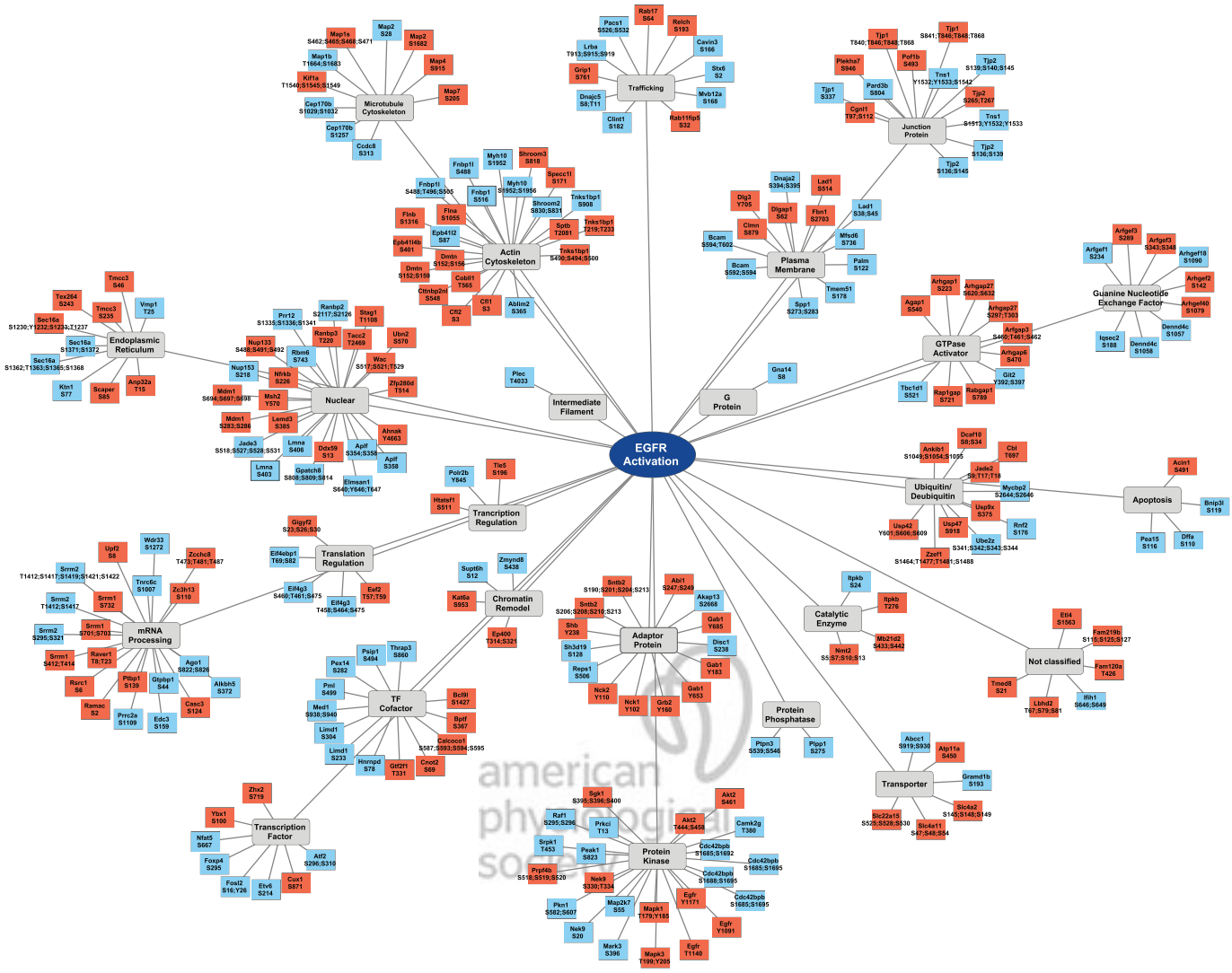

Figure 7. Mapping proteins with significant phosphorylation change by EGF to cellular structures or functions. The identified EGF-regulated phosphoproteins were mapped to Gene Ontology cellular component or molecular function terms (gray boxes) using Automated Bioinformatics Extractor (ABE, https://esbl.nhlbi.nih.gov/ABE/). Proteins with increased phosphorylation change at specific sites by EGF were labeled as red boxes. Proteins with decreased phosphorylation change at specific sites by EGF were labeled as blue boxes. Plotting was achieved in an Excel sheet, then exported and edited in Cytoscape. EGFR, epidermal growth factor receptor.

AQ: 21

the PI3K-AKT pathway were somewhat unexpected and indicated a potential regulatory role in protein translation. We cannot conclude from the present study that AKT is activated, as the sites of EGF-induced AKT2 phosphorylation differ from those typically associated with AKT activation, and the consequences of phosphorylation at these sites are unknown. However, our previous study demonstrated through immunoblotting that EGF, after a shorter incubation time of 5 min, induced AKT activation by increasing AKT1 phosphorylation at Thr308 and Ser473 (52). Nevertheless, the data point to the Gene Ontology Biological Process "regulation of translation" as a downstream component of AKT signaling (Fig. 4 and Table 3). Nineteen regulated phosphoproteins mapped to this Gene Ontology Biological Process term including three that are directly related to regulation of the translational process, viz. a double phosphopeptide (T57/T59) that increases in abundance in eukaryotic translation elongation factor 2 (EEF2), a double phosphopeptide (T69/S82) that decreases in abundance in eukaryotic translation initiation factor 4E binding protein 1 (EIF4EBP1), and eukaryotic translation initiation factor 4 γ 3 (EIF4G3), the first two of which have known functional effects on protein activity. Specifically, an increase in T57 phosphorylation of EEF2 is associated with inhibition of protein translation elongation (58). Second, a decrease in T69 phosphorylation of EIF4EBP1 increases binding of EIF4E, which is required for translation initiation (59). These phosphorylation effects on translational proteins predict a decrease in protein translation (Fig. 8), which is opposite to the expected effects of EGF seen in cancer cells with mutated EGFR (30, 60) in which the PI3K-AKT signaling pathway was found significantly activated.

Although EGF was found to activate the canonical MAPK signaling pathway (Supplemental Fig. S2*A*), our study did not find evidence of EGF activating the noncanonical MAPK signaling pathways of JNK (MAPK8, MAPK9, MAPK10) or p38 (MAPK11, MAPK12, MAPK13, MAPK14). In addition, there

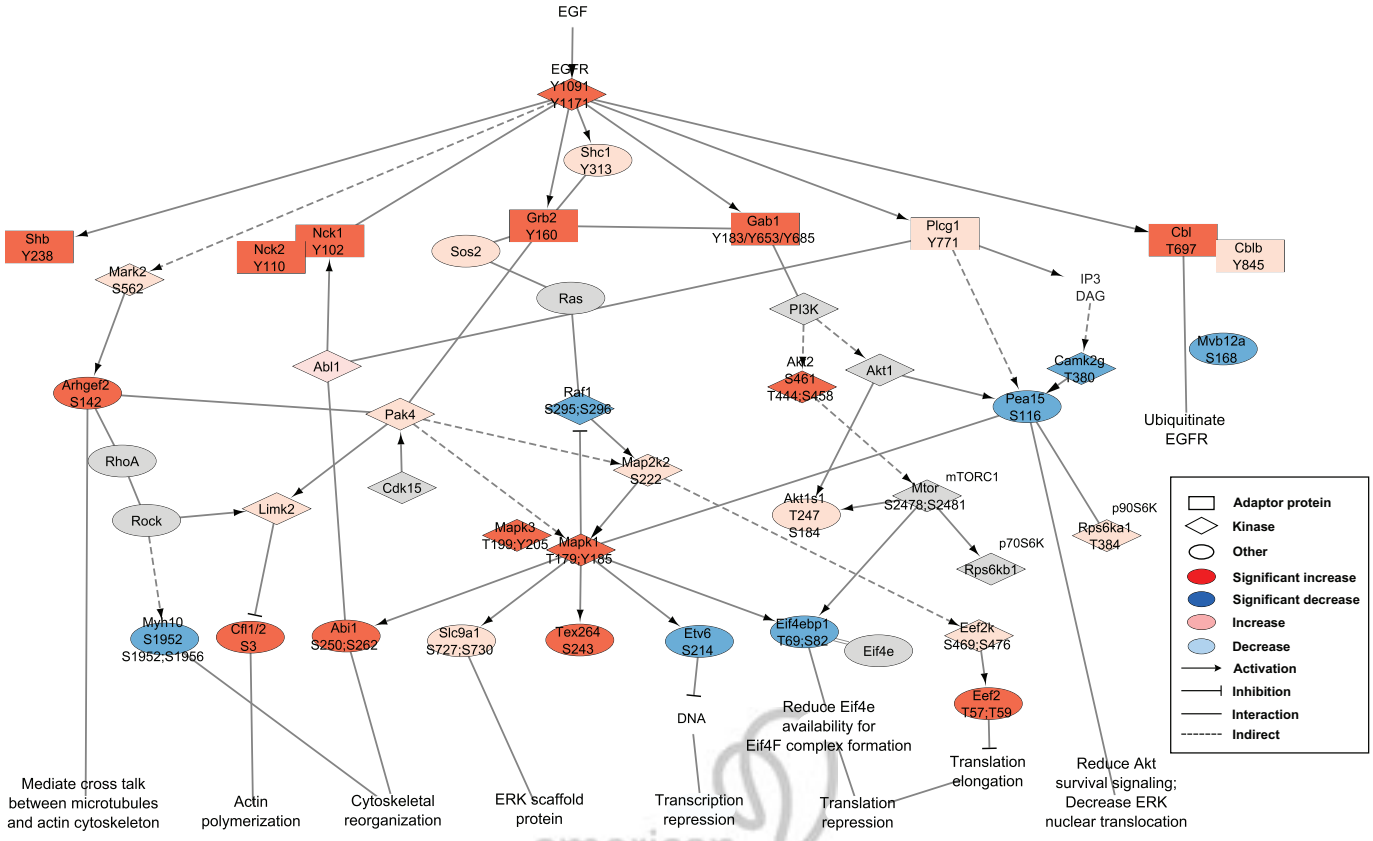

COLOR

Figure 8. A causal map summarizing the effects of EGF in native rat IMCD. The network of nodes (identified phosphosites) was connected by edges (directions of effect) based on literature search and phosphoproteomic data obtained from the present study. Nodes that are presented as red color (significantly increased phosphorylation by EGF) and blue color (significantly decreased phosphorylation by EGF) have both P value < 0.1 and $|\log_2(\text{EGF/Control})| > 0.3428$. Nodes that are presented as light red or light blue have a P value < 0.1 but with a $|\log_2(\text{EGF/Control})|$ value lower than the cut-off mark of 0.3428. Nodes that are presented as gray color are either not significantly changed or not identified in the present study. The mapping shows that following EGF stimulation, autophosphorylation of EGFR at Y1091 and Y1171 induces the tyrosine kinase activity of the receptor to phosphorylate several adaptor proteins that are known to interact with EGFR. Subsequent downstream effectors were found predominantly in activation of RAF-MEK-ERK signaling pathway, whereas effects on AKT-mTOR pathway lead to translation repression. EGF has also affected many proteins associated with cytoskeleton arrangement. Also shown are several ERK downstream effectors identified in the present study (ABI1, TEX264, ETV6, EIF4EBP1, RAF1). AKT, α serine/threonine-protein kinase; EGFR, epidermal growth factor receptor; IMCD, inner medullary collecting duct.

AQ: 22

were no observed phosphorylation changes in several ERK downstream effectors explicitly outlined in the KEGG MAPK signaling pathway (rno04010), such as the members of AP-1 complex (c-JUN, c-FOS, and ATF) or ELK1 (a nuclear target of ERK), or nonreceptor tyrosine kinases (including FES, JAK, ACK, SYK, TEC, FAK, SRC, and the CSK family of kinases). The activation of the transcription factor Stat3 in collecting duct cells of autosomal dominant polycystic kidney disease (ADPKD) has been reported, with this activation being enhanced by the coordinated signaling of both EGFR and cAMP, which promotes cyst formation (61). However, in native collecting duct cells, we found no evidence of modulation of JAK/STAT signaling by EGF (Supplemental Fig. S2*B*). These findings indicate a tightly regulated ERK signaling response to EGF stimulation in normal, native rat IMCD cells. Previous studies have identified PEA15 and SLC9A1 as ERK-binding proteins that likely regulate ERK activity, and both were detected in the current EGF-induced phosphoproteome. PEA15, also known as phosphoprotein enriched in Astrocytes 15, is known to interact with ERK, sequestering its cytoplasmic localization and signaling (62–64). In this study, EGF notably decreased PEA15 phosphorylation at Ser116, a site targeted by CAMK2 (65) and AKT1 (66), suggesting its interaction with ERK and potential influence on its subcellular targets. The Na^+/H^+ exchanger 1 (NHE1, gene symbol *Slc9a1*), which is known for its role in cell pH and volume regulation, also functions as a scaffold, interacting with ERK2 at its intracellular C-terminal tail (67). ERK2 phosphorylates NHE1, leading to reciprocal regulation of ERK phosphorylation. In our study, NHE1 showed increased phosphorylation on Ser727 and Ser730 (Fig. 8), both of which are ERK targets located between the D1 and D2 intrinsically disordered regions of hNHE1 (67). These interactions suggest that PEA15 and NHE1 play roles in fine-tuning ERK signaling.

The kidney collecting duct is a primary site of cyst formation in ADPKD (68). This condition is characterized by mislocated EGFR and various abnormalities in apical-basal (69, 70) and planar (71, 72) cell polarity. Our study suggests that EGF may play a role in regulating cell polarity and tight junction organization, which is significant in the context of ADPKD (70). These findings provide a rationale for

Table 7. *Nodes and edges for the causal map of EGF effects in IMCD*

Source	Target	Direction	Target Type	Net Target Activity	Source (PMID)
EGF	EGFR (Y1091/Y1171)	Up	Kinase	Increase	15901825
EGFR	Shc1 (Y313)	Up	Adaptor protein	Create binding motif for the SH2 domain of Grb2	23846654
EGFR	Grb2 (Y160)	Up	Adaptor protein	Recruit SOS through its SH3 domain	35507881
Sos2	Ras	NA	Small GTPase	SOS mediates the coupling of EGFR to Ras by inducing the exchange of GDP for GTP	11057895
Ras	Raf1 (S295;S296)	NA	Kinase	Tyrosine phosphorylation of Raf1 is essential for its recruitment to the plasma membrane and activation	7542586 8622647
Raf1	Map2k2 (S222)	Up	Kinase	Increase	8157000 22177953
Map2k2	Mapk1 (T179;Y185) Mapk3 (T199;Y205)	Up	Kinase	Increase	9677429
Mapk1 Mapk3	Raf1 (S295;S296)	Down	Kinase	Increase	15664191 15642359
Mapk1 Mapk3	Abi1 (S250;S262)	Up	Abl interactor	Cytoskeletal reorganization	21419341
Mapk1	Slc9a1 (S727;S730)	Up	A major regulator of pH and volume	Increase; serve as a membrane scaffold of ERK2 regulates its phosphorylation	27083547
Mapk3	Etv6 (S214)	Down	Transcriptional repressor	Transcription repression	15060146
Mapk1 Mapk3	Tex264 (S243)	Up	ER-resident protein with roles in both autophagy and DNA repair	NA	24719451
Mapk1 Mapk3	Eif4ebp1 (T69;S82)	Down	Repressor of translation initiation	Increase binding to Eif4e	10942774 PhosphoSite
EGFR	Gab1 (Y653/Y685)	Up	Adaptor protein	Recruit downstream signaling elements, SHP2, PI3K PLC-g, CRK	9890893
Grb2	Gab1 (Y653/Y685)	Interaction	Adaptor protein	Act as a Grb2-associated docking protein for several SH2-containing proteins	8596638
Gab1	PI3K	–	Kinase	NA	16687399
PI3K	Akt1	–	Kinase	NA	10908564
PI3K	Akt2 (S461, S444;S458)	Up	Kinase	NA	10908564 22261254
Akt1	Pea15 (S116)	Down	ERK-binding phosphoprotein	Decrease Akt survival signaling	12808093
Akt	mTOR (S2478;S2481)	–	Kinase	Slightly increase Mtor S2481 phosphorylation	10702316 20022946
Mtor	Akt1s1 (S184)	Up	Raptor-interacting protein, subunit of mTORC1	Increase phosphorylation and associate with 14-3-3, relieve its inhibitor activity on mTORC1	17517883 18372248 21914810
Akt1	Akt1s1 (T247)	Up	Raptor-interacting protein, subunit of mTORC1	Increase phosphorylation and associate with 14-3-3, relieve its inhibitor activity on mTORC1	12524439 17277771 17386266
Mtor	Eif4ebp1 (T69;S82)	Down	Repressor of translation initiation	Increase binding to Eif4e	10702316 20804212
Mtor	Rps6kb1	–	p70S6K Serine/threonine-protein kinase	Dephosphorylation of Rps6b1	10702316 20804212
Map2k2	Eef2K (S469)	Up	Kinase	Eef2k is a key convergence point downstream of PI3K and MEK	19651622 35513296
Eef2k	Eef2 (T57)	Up	Translation elongation factor	Reduce translation elongation	2753158 29800565
EGFR	Plcg1 (Y771)	–	Catalytic enzyme for DAG and IP3 production	NA	1708307
EGFR	Camk2g (T380)	Down	Kinase	NA	This paper
Plcg1	Pea15 (S116)	Down	ERK-binding phosphoprotein	Decrease ERK nuclear translocation	21285289
Camk2	Pea15 (S116)	Down	ERK-binding phosphoprotein	S116 of Pea15 is a Camk2 target site	9721757
Pea15	Mapk1 Mapk3	Interaction	Kinase	Increase binding ERKs and prevent their nuclear localization, protects ERK2 from dephosphorylation	11702783 23575685
Pea15	Rps6ka1	Interaction	Kinase	Regulate p90 ribosomal S6 kinase (RSK) activity	12796492
EGF	Rps6ka1 (T384)	Up	Kinase	NA	This paper
EGFR	Shb (Y238)	Up	Adaptor protein	Essential for Shb binding of p120-RasGAP	32060095
EGFR	Cbl (T697)	Up	E3 ubiquitin ligase and signaling adaptor	NA	This paper
EGFR	Nck1 (Y102)	Up	Adaptor protein	NA	1448108
Abi1	Abl	Interaction	Kinase	Interact with Abl and modulate kinase activity	20841568

Continued

Table 7.— *Continued*

Source	Target	Direction	Target Type	Net Target Activity	Source (PMID)
Abl1	Nck1 (Y102)	Up	Adaptor protein	Downregulate p38 MAPK activity	22327338
Abl1	Plcg1 (Y771)	Interaction	Catalytic enzyme	Negatively regulate Plcg1	12652307
Limk2	Cfl1/2 (S3)	Up	Actin-modulating protein	Inhibit Cfl1/2, actin polymerization	9655397 10436159
Rock	Limk2	Up	Kinase	Increase	10436159
Cdk15	Pak4 (S293)	Up	Kinase	Cdk15 can phosphorylation Pak4 at S293	34262144
Pak4	Limk2	Up	Kinase	Increase	24297048
Pak4	Mapk1 Mapk3	Up	Kinase	Increases ERK phosphorylation	34262144
Pak4	Mpk2k1/2	Up	Kinase	Increase MEK phosphorylation	34262144
Pak4	Grb2	Interaction	Adaptor protein	Interact with GRB2	12529371
Pak4	Arhgef2	Interaction	Rho GEF	Pak4 acts as a crucial regulator of Arhgef2	15827085
EGF	Mark2 (S562)	Up	Kinase	Participate in mitotic progression, cell cycle progression	27281782 35780183
Mark2	Arhgef2 (S143)	Up	Rho GEF	Regulate its interaction with microtubules, contribute to cell polarity	21513698
Arhgef2	RhoA	NA	Rho GTPase	Promote nucleotide exchange on RhoA	11912491
NA	Myh10 (S1956/S1956;S1962)	Down	Actin motor protein	Enhance filament assembly	30087119
NA	Mvb12a (S168)	Down	Component of ESCRT-I complex, required for the sorting of endocytic ubiquitinated cargos into multivesicular bodies	May participate in the ligand-mediated internalization and downregulation of EGF receptor by recruitment of Cbl	16895919 18005716

EGF, epidermal growth factor; IMCD, inner medullary collecting duct. -, no significant change; NA, not available.

investigating EGF pathway modulators as potential therapies for ADPKD (73).

Interestingly, although EGF negatively regulates water (7–12) and ion (3, 4, 6, 18, 20, 74) transport across the collecting duct epithelium, none of the responsive phosphoproteins identified were transporters directly involved in mediating water or ion transport. This suggests that EGF-mediated phosphorylation likely alters the function of other proteins that indirectly regulate these transporters. Our study, along with previous research (52), demonstrated that EGF can increase intracellular calcium levels in IMCD cells, likely by activating phospholipase C (PLCγ) and elevating intracellular IP_3 levels (75). Several proteins involved in regulating IP_3 production, such as ITPKB, PLCB3, and PLCB4, also exhibited phosphorylation changes in response to EGF (Supplemental Table S2). Since AVP increases water permeability through

COLOR

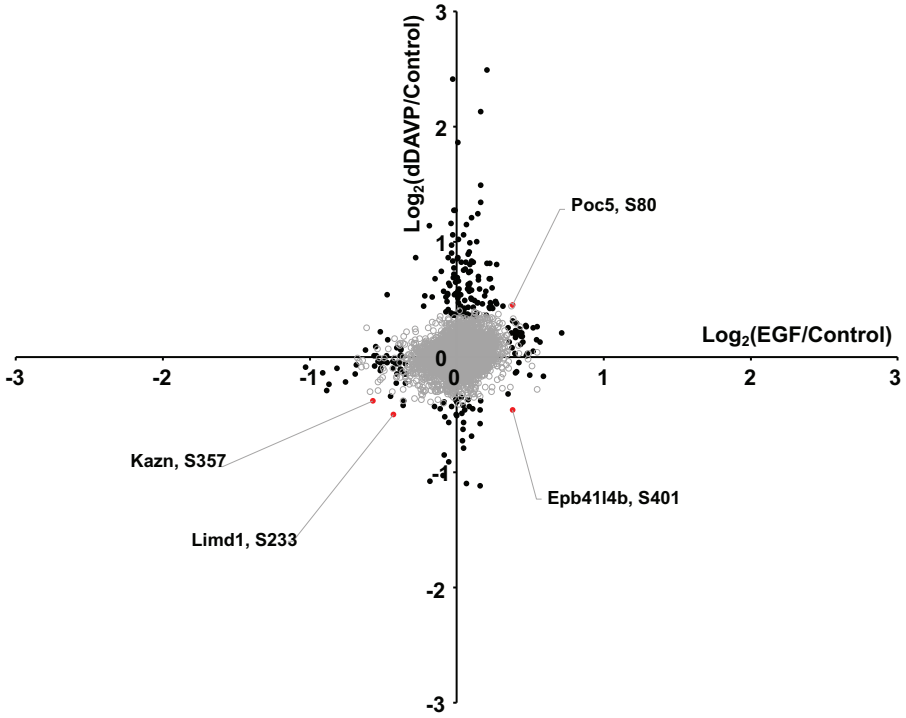

Figure 9. A scatter plot comparing the phosphorylation change of the same phosphosites identified in both EGF (current) and dDAVP (previous study). To compare the current dataset with the previous dDAVP dataset (53), we first converted the *t* test *P* values of all identified phosphosites in the current study to the P_{joint} value that was used in the previous study (53). *X*-axis depicts log_2(EGF/Control) values and *y*-axis depicts log_2(dDAVP/Control) of the same phosphosites. The black circles shows the phosphosites that are significantly changed in either EGF or dDAVP study. The red circles show the phosphosites that are significantly changed in both EGF and dDAVP studies. Among these, EPB41|4B (S401) exhibits an opposite change in phosphorylation in response to EGF and dDAVP stimulation, whereas POC5 (S80) was increased, and KAZN (S357) and LIMD1 (S233) were decreased, in phosphorylation in both EGF and dDAVP studies. EGF, epidermal growth factor.

V2R-adenylyl cyclase-cAMP signaling, and adenylyl cyclase 6, present in collecting duct cells, is calcium-inhibitable (76–79), it is possible that EGF-induced calcium increase could play a role in EGF-mediated downregulation of water permeability in IMCD cells.

Perspectives and Significance

Numerous studies have highlighted the prevalence of EGF-induced activation of the ERK and PI3K-AKT pathways in proliferative cancer cells or disease tissues. However, there is comparatively little information about EGF actions in normal epithelia. In this study, we generated a comprehensive EGF-induced phosphoproteomic dataset in native kidney collecting duct cells from normal rats. Bioinformatic analysis revealed consistent activation of the classical MAPK signaling pathway via the RAS-MEK-RAF cascade, alongside the inactivation of several PI3K-AKT-MTOR downstream proteins necessary for the protein translation machinery that otherwise would promote cell growth in physiologically quiescent collecting duct cells. In additionlly, the study suggests a potential role for EGF in regulating cell polarity, which could be significant in the context of autosomal dominant polycystic kidney disease (ADPKD). This dataset serves as a valuable resource for designing future studies investigating the actions of EGF.

AQ: 15

DATA AVAILABILITY

Data will be made available upon reasonable request.

AQ: 16

SUPPLEMENTAL MATERIAL

Supplemental Figs. S1 and S2, Supplemental Tables S1 and S2, and Supplemental Video S1: https://figshare.com/s/1d8393bce523c2d88efe.

ACKNOWLEDGMENTS

Mass spectrometry was done in the National Heart, Lung, and Blood Institute (NHLBI) Proteomics Core (Drs. Marjan Gucek and Guanghui Wang). Imaging of intracellular Ca^{2+} was done in the NHLBI Light Microscopy Core (Drs. Christian Combs and Daniella Malide).

Present address of K. Limbutara: Division of Nephrology and Renal Replacement Therapy, Department of Internal Medicine, Faculty of Medicine Vajira Hospital, Navamindradhiraj University, Bangkok, Thailand.

AQ: 17

GRANTS

The work was primarily funded by the Division of Intramural Research, National Heart, Lung, and Blood Institute under Project Nos. ZIA-HL001285 and ZIA-HL006129 (to M.A.K.).

AQ: 18

DISCLOSURES

No conflicts of interest, financial or otherwise, are declared by the authors.

AQ: 19

AUTHOR CONTRIBUTIONS

M.A.K. conceived and designed research; C.-L.C. and E.T.K. performed experiments; N.U.J., S.-M.O., and K.L. analyzed data.

REFERENCES

1. **Chen L**, **Chou CL**, **Knepper MA.** A comprehensive map of mRNAs and their isoforms across all 14 renal tubule segments of mouse. *J Am Soc Nephrol* 32: 897–912, 2021. doi:10.1681/ASN.2020101406.
2. **Muto S**, **Furuya H**, **Tabei K**, **Asano Y.** Site and mechanism of action of epidermal growth factor in rabbit cortical collecting duct. *Am J Physiol Renal Physiol* 260: F163–F169, 1991. doi:10.1152/ajprenal.1991.260.2.F163.
3. **Ookawara S**, **Tabei K**, **Furuya H**, **Asano Y.** The effect of EGF on electrolyte transport is mediated by tyrosine kinases in the rabbit cortical collecting duct. *Miner Electrolyte Metab* 25: 191–198, 1999. doi:10.1159/000057444.
4. **Vehaskari VM**, **Hering-Smith KS**, **Moskowitz DW**, **Weiner ID**, **Hamm LL.** Effect of epidermal growth factor on sodium transport in the cortical collecting tubule. *Am J Physiol Renal Physiol* 256: F803–F809, 1989. doi:10.1152/ajprenal.1989.256.5.F803.
5. **Vehaskari VM**, **Herndon J**, **Hamm LL.** Mechanism of sodium transport inhibition by epidermal growth factor in cortical collecting ducts. *Am J Physiol Renal Physiol* 261: F896–F903, 1991. doi:10.1152/ajprenal.1991.261.5.F896.
6. **Warden DH**, **Stokes JB.** EGF and PGE2 inhibit rabbit CCD Na+ transport by different mechanisms: PGE2 inhibits Na(+)-K+ pump. *Am J Physiol Renal Physiol* 264: F670–F677, 1993. doi:10.1152/ajprenal.1993.264.4.F670.
7. **Breyer MD**, **Jacobson HR**, **Breyer JA.** Epidermal growth factor inhibits the hydroosmotic effect of vasopressin in the isolated perfused rabbit cortical collecting tubule. *J Clin Invest* 82: 1313–1320, 1988. doi:10.1172/JCI113732.
8. **Cheung PW**, **Nomura N**, **Nair AV**, **Pathomthongtaweechai N**, **Ueberdiek L**, **Lu HA**, **Brown D**, **Bouley R.** EGF receptor inhibition by Erlotinib increases aquaporin 2-mediated renal water reabsorption. *J Am Soc Nephrol* 27: 3105–3116, 2016. doi:10.1681/ASN.2015080903.
9. **Gow CB**, **Phillips PA**, **Chandler KD**, **Moore GP.** Hormonal, fluid, and electrolyte responses of sheep during chronic intravenous infusion of epidermal growth factor. *Am J Physiol Regul Integr Comp Physiol* 265: R203–R210, 1993. doi:10.1152/ajpregu.1993.265.1.R203.
10. **Grant SL**, **Gow CB**, **Phillips PA.** Epidermal growth factor and fluid and electrolyte balance in the rat. *Am J Physiol Regul Integr Comp Physiol* 272: R1853–R1861, 1997. doi:10.1152/ajpregu.1997.272.6.R1853.
11. **Phillips PA**, **Grant SL**, **Davidson AF**, **Risvanis J**, **Stephenson J**, **Gow CB.** Epidermal growth factor antagonizes vasopressin in vivo and in vitro. *Kidney Int* 45: 1028–1036, 1994. doi:10.1038/ki.1994.139.
12. **Chou CL**, **Limbutara K**, **Kao AR**, **Clark JZ**, **Nein EH**, **Raghuram V**, **Knepper MA.** Collecting duct water permeability inhibition by EGF is associated with decreased cAMP, PKA activity and AQP2 phosphorylation at Ser269. *Am J Physiol Renal Physiol* 326: F545–F559, 2024. doi:10.1152/ajprenal.00197.2023.
13. **Grant SL**, **Phillips PA**, **Gow CB.** Interaction between epidermal growth factor and arginine vasopressin in renal medullary membranes. *Clin Exp Pharmacol Physiol* 21: 243–247, 1994. doi:10.1111/j.1440-1681.1994.tb02506.x.
14. **Heasley LE**, **Senkfor SI**, **Winitz S**, **Strasheim A**, **Teitelbaum I**, **Berl T.** Hormonal regulation of MAP kinase in cultured rat inner medullary collecting tubule cells. *Am J Physiol Renal Physiol* 267: F366–F373, 1994. doi:10.1152/ajprenal.1994.267.3.F366.
15. **Teitelbaum I.** Cyclic adenosine monophosphate and diacylglycerol. Mutually inhibitory second messengers in cultured rat inner medullary collecting duct cells. *J Clin Invest* 86: 46–51, 1990. doi:10.1172/JCI114713.
16. **Falin R**, **Veizis IE**, **Cotton CU.** A role for ERK1/2 in EGF- and ATP-dependent regulation of amiloride-sensitive sodium absorption. *Am J Physiol Cell Physiol* 288: C1003–C1011, 2005. doi:10.1152/ajpcell.00213.2004.
17. **Falin RA**, **Cotton CU.** Acute downregulation of ENaC by EGF involves the PY motif and putative ERK phosphorylation site. *J Gen Physiol* 130: 313–328, 2007. doi:10.1085/jgp.200709775.
18. **Gekle M**, **Freudinger R**, **Mildenberger S**, **Silbernagl S.** Rapid actions of aldosterone on cells from renal epithelium: the possible role of EGF-receptor signaling. *Steroids* 67: 499–504, 2002. doi:10.1016/s0039-128x(01)00183-0.

19. **Levchenko V**, **Zheleznova NN**, **Pavlov TS**, **Vandewalle A**, **Wilson PD**, **Staruschenko A.** EGF and its related growth factors mediate sodium transport in mpkCCDc14 cells via ErbB2 (neu/HER-2) receptor. *J Cell Physiol* 223: 252–259, 2010. doi:10.1002/jcp.22033.
20. **Shen JP**, **Cotton CU.** Epidermal growth factor inhibits amiloride-sensitive sodium absorption in renal collecting duct cells. *Am J Physiol Renal Physiol* 284: F57–F64, 2003. doi:10.1152/ajprenal.00028.2002.
21. **Arima H**, **Cheetham T**, **Christ-Crain M**, **Cooper D**, **Drummond J**, **Gurnell M**, **Levy M**, **McCormack A**, **Newell-Price J**, **Verbalis JG**, **Wass J**; **Working Group for Renaming Diabetes Insipidus.** Changing the name of diabetes insipidus: a position statement of the working group for renaming diabetes insipidus. *J Clin Endocrinol Metab* 108: 1–3, 2022. doi:10.1210/clinem/dgac547.
22. **Sung CC**, **Chen L**, **Limbutara K**, **Jung HJ**, **Gilmer GG**, **Yang CR**, **Lin SH**, **Khositseth S**, **Chou CL**, **Knepper MA.** RNA-Seq and protein mass spectrometry in microdissected kidney tubules reveal signaling processes initiating lithium-induced nephrogenic diabetes insipidus. *Kidney Int* 96: 363–377, 2019. doi:10.1016/j.kint.2019.02.015.
23. **Chen X**, **Guo D**, **Zhu Y**, **Xian F**, **Liu S**, **Wu L**, **Lou X.** Nuclear phosphoproteomics analysis reveals that CDK1/2 are involved in EGF-regulated constitutive pre-mRNA splicing in MDA-MB-468 cells. *J Proteomics* 141: 77–84, 2016. doi:10.1016/j.jprot.2016.04.031.
24. **Olsen JV**, **Blagoev B**, **Gnad F**, **Macek B**, **Kumar C**, **Mortensen P**, **Mann M.** Global, in vivo, and site-specific phosphorylation dynamics in signaling networks. *Cell* 127: 635–648, 2006. doi:10.1016/j.cell.2006.09.026.
25. **Yi L**, **Shi T**, **Gritsenko MA**, **X'Avia Chan CY**, **Fillmore TL**, **Hess BM**, **Swensen AC**, **Liu T**, **Smith RD**, **Wiley HS**, **Qian WJ.** Targeted quantification of phosphorylation dynamics in the context of EGFR-MAPK pathway. *Anal Chem* 90: 5256–5263, 2018. doi:10.1021/acs.analchem.8b00071.
26. **Zhang X**, **Belkina N**, **Jacob HK**, **Maity T**, **Biswas R**, **Venugopalan A**, **Shaw PG**, **Kim MS**, **Chaerkady R**, **Pandey A**, **Guha U.** Identifying novel targets of oncogenic EGF receptor signaling in lung cancer through global phosphoproteomics. *Proteomics* 15: 340–355, 2015. doi:10.1002/pmic.201400315.
27. **Eguchi A**, **Olsen JV.** Phosphoproteomic investigation of targets of protein phosphatases in EGFR signaling. *Sci Rep* 14: 7908, 2024. doi:10.1038/s41598-024-58619-1.
28. **Erba EB**, **Matthiesen R**, **Bunkenborg J**, **Schulze WX**, **Di Stefano P**, **Cabodi S**, **Tarone G**, **Defilippi P**, **Jensen ON.** Quantitation of multisite EGF receptor phosphorylation using mass spectrometry and a novel normalization approach. *J Proteome Res* 6: 2768–2785, 2007. doi:10.1021/pr060675m.
29. **Jorissen RN**, **Walker F**, **Pouliot N**, **Garrett TP**, **Ward CW**, **Burgess AW.** Epidermal growth factor receptor: mechanisms of activation and signalling. *Exp Cell Res* 284: 31–53, 2003. doi:10.1016/s0014-4827(02)00098-8.
30. **Sordella R**, **Bell DW**, **Haber DA**, **Settleman J.** Gefitinib-sensitizing EGFR mutations in lung cancer activate anti-apoptotic pathways. *Science* 305: 1163–1167, 2004. doi:10.1126/science.1101637.
31. **Palanisamy S**, **Xue C**, **Ishiyama S**, **Naga Prasad SV**, **Gabrielson K.** GPCR-ErbB transactivation pathways and clinical implications. *Cell Signal* 86: 110092, 2021. doi:10.1016/j.cellsig.2021.110092.
32. **Wang W**, **Qiao Y**, **Li Z.** New insights into modes of GPCR activation. *Trends Pharmacol Sci* 39: 367–386, 2018. doi:10.1016/j.tips.2018.01.001.
33. **Bisson N**, **James DA**, **Ivosev G**, **Tate SA**, **Bonner R**, **Taylor L**, **Pawson T.** Selected reaction monitoring mass spectrometry reveals the dynamics of signaling through the GRB2 adaptor. *Nat Biotechnol* 29: 653–658, 2011. doi:10.1038/nbt.1905.
34. **Pawson T.** Dynamic control of signaling by modular adaptor proteins. *Curr Opin Cell Biol* 19: 112–116, 2007. doi:10.1016/j.ceb.2007.02.013.
35. **Zheng Y**, **Zhang C**, **Croucher DR**, **Soliman MA**, **St-Denis N**, **Pasculescu A**, **Taylor L**, **Tate SA**, **Hardy WR**, **Colwill K**, **Dai AY**, **Bagshaw R**, **Dennis JW**, **Gingras AC**, **Daly RJ**, **Pawson T.** Temporal regulation of EGF signalling networks by the scaffold protein Shc1. *Nature* 499: 166–171, 2013. doi:10.1038/nature12308.
36. **Perez-Riverol Y**, **Csordas A**, **Bai J**, **Bernal-Llinares M**, **Hewapathirana S**, **Kundu DJ**, **Inuganti A**, **Griss J**, **Mayer G**, **Eisenacher M**, **Perez E**, **Uszkoreit J**, **Pfeuffer J**, **Sachsenberg T**, **Yilmaz S**, **Tiwary S**, **Cox J**, **Audain E**, **Walzer M**, **Jarnuczak AF**, **Ternent T**, **Brazma A**, **Vizcaino JA.** The PRIDE database and related tools and resources in 2019: improving support for quantification data. *Nucleic Acids Res* 47: D442–D450, 2019. doi:10.1093/nar/gky1106.
37. **Saethang T**, **Hodge K**, **Yang CR**, **Zhao Y**, **Kimkong I**, **Knepper MA**, **Pisitkun T.** PTM-Logo: a program for generation of sequence logos based on position-specific background amino-acid probabilities. *Bioinformatics* 35: 5313–5314, 2019. doi:10.1093/bioinformatics/btz568.
38. **Boeri Erba E**, **Bergatto E**, **Cabodi S**, **Silengo L**, **Tarone G**, **Defilippi P**, **Jensen ON.** Systematic analysis of the epidermal growth factor receptor by mass spectrometry reveals stimulation-dependent multisite phosphorylation. *Mol Cell Proteomics* 4: 1107–1121, 2005. doi:10.1074/mcp.M500070-MCP200.
39. **Ahmed Z**, **Lin CC**, **Suen KM**, **Melo FA**, **Levitt JA**, **Suhling K**, **Ladbury JE.** Grb2 controls phosphorylation of FGFR2 by inhibiting receptor kinase and Shp2 phosphatase activity. *J Cell Biol* 200: 493–504, 2013. doi:10.1083/jcb.201204106.
40. **Lehr S**, **Kotzka J**, **Herkner A**, **Klein E**, **Siethoff C**, **Knebel B**, **Noelle V**, **Bruning JC**, **Klein HW**, **Meyer HE**, **Krone W**, **Muller-Wieland D.** Identification of tyrosine phosphorylation sites in human Gab-1 protein by EGF receptor kinase in vitro. *Biochemistry* 38: 151–159, 1999. doi:10.1021/bi9818265.
41. **Koch H**, **Wilhelm M**, **Ruprecht B**, **Beck S**, **Frejno M**, **Klaeger S**, **Kuster B.** Phosphoproteome profiling reveals molecular mechanisms of growth-factor-mediated kinase inhibitor resistance in EGFR-overexpressing cancer cells. *J Proteome Res* 15: 4490–4504, 2016. doi:10.1021/acs.jproteome.6b00621.
42. **Roh MH**, **Margolis B.** Composition and function of PDZ protein complexes during cell polarization. *Am J Physiol Renal Physiol* 285: F377–F387, 2003. doi:10.1152/ajprenal.00086.2003.
43. **Fanning AS**, **Anderson JM.** PDZ domains: fundamental building blocks in the organization of protein complexes at the plasma membrane. *J Clin Invest* 103: 767–772, 1999. doi:10.1172/JCI6509.
44. **Kim SK.** Polarized signaling: basolateral receptor localization in epithelial cells by PDZ-containing proteins. *Curr Opin Cell Biol* 9: 853–859, 1997. doi:10.1016/s0955-0674(97)80088-9.
45. **Brône B**, **Eggermont J.** PDZ proteins retain and regulate membrane transporters in polarized epithelial cell membranes. *Am J Physiol Cell Physiol* 288: C20–C29, 2005. doi:10.1152/ajpcell.00368.2004.
46. **Brown D**, **Breton S.** Sorting proteins to their target membranes. *Kidney Int* 57: 816–824, 2000. doi:10.1046/j.1523-1755.2000.00920.x.
47. **Poll BG**, **Leo KT**, **Deshpande V**, **Jayatissa N**, **Pisitkun T**, **Park E**, **Yang CR**, **Raghuram V**, **Knepper MA.** A resource database for protein kinase substrate sequence-preference motifs based on large-scale mass spectrometry data. *Cell Commun Signal* 22: 137, 2024. doi:10.1186/s12964-023-01436-2.
48. **Park E**, **Yang CR**, **Raghuram V**, **Chen L**, **Chou CL**, **Knepper MA.** Using CRISPR-Cas9/phosphoproteomics to identify substrates of calcium/calmodulin dependent kinase 2δ. *J Biol Chem* 299: 105371, 2023. doi:10.1016/j.jbc.2023.105371.
49. **Mehta YR**, **Lewis SA**, **Leo KT**, **Chen L**, **Park E**, **Raghuram V**, **Chou CL**, **Yang CR**, **Kikuchi H**, **Khundmiri S**, **Poll BG**, **Knepper MA.** ADPKD-"omics": determinants of cyclic AMP levels in renal epithelial cells. *Kidney Int* 101: 47–62, 2022. doi:10.1016/j.kint.2021.10.014.
50. **Bansal AD**, **Hoffert JD**, **Pisitkun T**, **Hwang S**, **Chou CL**, **Boja ES**, **Wang G**, **Knepper MA.** Phosphoproteomic profiling reveals vasopressin-regulated phosphorylation sites in collecting duct. *J Am Soc Nephrol* 21: 303–315, 2010. doi:10.1681/ASN.2009070728.
51. **Wu S**, **Birnbaumer M**, **Guan Z.** Phosphorylation analysis of G protein-coupled receptor by mass spectrometry: identification of a phosphorylation site in V2 vasopressin receptor. *Anal Chem* 80: 6034–6037, 2008. doi:10.1021/ac8008548.
52. **Han JS**, **Maeda Y**, **Ecelbarger C**, **Knepper MA.** Vasopressin-independent regulation of collecting duct water permeability. *Am J Physiol Renal Physiol* 266: F139–F146, 1994. doi:10.1152/ajprenal.1994.266.1.F139.
53. **Deshpande V**, **Kao A**, **Raghuram V**, **Datta A**, **Chou CL**, **Knepper MA.** Phosphoproteomic identification of vasopressin V2 receptor-dependent signaling in the renal collecting duct. *Am J Physiol Renal Physiol* 317: F789–F804, 2019. doi:10.1152/ajprenal.00281.2019.
54. **Pisitkun T**, **Jacob V**, **Schleicher SM**, **Chou CL**, **Yu MJ**, **Knepper MA.** Akt and ERK1/2 pathways are components of the vasopressin signaling network in rat native IMCD. *Am J Physiol Renal Physiol* 295: F1030–F1043, 2008. doi:10.1152/ajprenal.90339.2008.

J_ID: AJPRENAL ART NO: F-00182-2024 Date: 20-November-24 20:25 Page: 19 Total Pages: 21 ini: 6//EP

55. **Amit I**, **Citri A**, **Shay T**, **Lu Y**, **Katz M**, **Zhang F**, **Tarcic G**, **Siwak D**, **Lahad J**, **Jacob-Hirsch J**, **Amariglio N**, **Vaisman N**, **Segal E**, **Rechavi G**, **Alon U**, **Mills GB**, **Domany E**, **Yarden Y.** A module of negative feedback regulators defines growth factor signaling. *Nat Genet* 39: 503–512, 2007. doi:10.1038/ng1987.
56. **Breyer MD**, **Redha R**, **Breyer JA.** Segmental distribution of epidermal growth factor binding sites in rabbit nephron. *Am J Physiol Renal Physiol* 259: F553–F558, 1990. doi:10.1152/ajprenal.1990.259.4.F553.
57. **Nouwen EJ**, **De Broe ME.** EGF and TGF-α in the human kidney: identification of octopal cells in the collecting duct. *Kidney Int* 45: 1510–1521, 1994. doi:10.1038/ki.1994.198.
58. **Hizli AA**, **Chi Y**, **Swanger J**, **Carter JH**, **Liao Y**, **Welcker M**, **Ryazanov AG**, **Clurman BE.** Phosphorylation of eukaryotic elongation factor 2 (eEF2) by cyclin A-cyclin-dependent kinase 2 regulates its inhibition by eEF2 kinase. *Mol Cell Biol* 33: 596–604, 2013. doi:10.1128/MCB.01270-12.
59. **Lekmine F**, **Sassano A**, **Uddin S**, **Smith J**, **Majchrzak B**, **Brachmann SM**, **Hay N**, **Fish EN**, **Platanias LC.** Interferon-γ engages the p70 S6 kinase to regulate phosphorylation of the 40S S6 ribosomal protein. *Exp Cell Res* 295: 173–182, 2004. doi:10.1016/j.yexcr.2003.12.021.
60. **Huang PH**, **Mukasa A**, **Bonavia R**, **Flynn RA**, **Brewer ZE**, **Cavenee WK**, **Furnari FB**, **White FM.** Quantitative analysis of EGFRvIII cellular signaling networks reveals a combinatorial therapeutic strategy for glioblastoma. *Proc Natl Acad Sci USA* 104: 12867–12872, 2007. doi:10.1073/pnas.0705158104.
61. **Talbot JJ**, **Song X**, **Wang X**, **Rinschen MM**, **Doerr N**, **LaRiviere WB**, **Schermer B**, **Pei YP**, **Torres VE**, **Weimbs T.** The cleaved cytoplasmic tail of polycystin-1 regulates Src-dependent STAT3 activation. *J Am Soc Nephrol* 25: 1737–1748, 2014. doi:10.1681/ASN.2013091026.
62. **Mace PD**, **Wallez Y**, **Egger MF**, **Dobaczewska MK**, **Robinson H**, **Pasquale EB**, **Riedl SJ.** Structure of ERK2 bound to PEA-15 reveals a mechanism for rapid release of activated MAPK. *Nat Commun* 4: 1681, 2013. doi:10.1038/ncomms2687.
63. **Formstecher E**, **Ramos JW**, **Fauquet M**, **Calderwood DA**, **Hsieh JC**, **Canton B**, **Nguyen XT**, **Barnier JV**, **Camonis J**, **Ginsberg MH**, **Chneiweiss H.** PEA-15 mediates cytoplasmic sequestration of ERK MAP kinase. *Dev Cell* 1: 239–250, 2001. doi:10.1016/s1534-5807(01)00035-1.
64. **Vaidyanathan H**, **Opoku-Ansah J**, **Pastorino S**, **Renganathan H**, **Matter ML**, **Ramos JW.** ERK MAP kinase is targeted to RSK2 by the phosphoprotein PEA-15. *Proc Natl Acad Sci USA* 104: 19837–19842, 2007. doi:10.1073/pnas.0704514104.
65. **Kubes M**, **Cordier J**, **Glowinski J**, **Girault JA**, **Chneiweiss H.** Endothelin induces a calcium-dependent phosphorylation of PEA-15 in intact astrocytes: identification of Ser104 and Ser116 phosphorylated, respectively, by protein kinase C and calcium/calmodulin kinase II in vitro. *J Neurochem* 71: 1307–1314, 1998. doi:10.1046/j.1471-4159.1998.71031307.x.
66. **Trencia A**, **Perfetti A**, **Cassese A**, **Vigliotta G**, **Miele C**, **Oriente F**, **Santopietro S**, **Giacco F**, **Condorelli G**, **Formisano P**, **Beguinot F.** Protein kinase B/Akt binds and phosphorylates PED/PEA-15, stabilizing its antiapoptotic action. *Mol Cell Biol* 23: 4511–4521, 2003. doi:10.1128/MCB.23.13.4511-4521.2003.
67. **Hendus-Altenburger R**, **Pedraz-Cuesta E**, **Olesen CW**, **Papaleo E**, **Schnell JA**, **Hopper JT**, **Robinson CV**, **Pedersen SF**, **Kragelund BB.** The human Na^+/H^+ exchanger 1 is a membrane scaffold protein for extracellular signal-regulated kinase 2. *BMC Biol* 14: 31, 2016. doi:10.1186/s12915-016-0252-7.
68. **Grantham JJ.** Mechanisms of progression in autosomal dominant polycystic kidney disease. *Kidney Int Suppl* 63: S93–97, 1997.
69. **Du J**, **Wilson PD.** Abnormal polarization of EGF receptors and autocrine stimulation of cyst epithelial growth in human ADPKD. *Am J Physiol Cell Physiol* 269: C487–495, 1995. doi:10.1152/ajpcell.1995.269.2.C487.
70. **Wilson PD.** Epithelial cell polarity and disease. *Am J Physiol Renal Physiol* 272: F434–F442, 1997. doi:10.1152/ajprenal.1997.272.4.F434.
71. **Luyten A**, **Su X**, **Gondela S**, **Chen Y**, **Rompani S**, **Takakura A**, **Zhou J.** Aberrant regulation of planar cell polarity in polycystic kidney disease. *J Am Soc Nephrol* 21: 1521–1532, 2010. doi:10.1681/ASN.2010010127.
72. **Papakrivopoulou E**, **Jafree DJ**, **Dean CH**, **Long DA.** The biological significance and implications of planar cell polarity for nephrology. *Front Physiol* 12: 599529, 2021. doi:10.3389/fphys.2021.599529.
73. **Capuano I**, **Buonanno P**, **Riccio E**, **Amicone M**, **Pisani A.** Therapeutic advances in ADPKD: the future awaits. *J Nephrol* 35: 397–415, 2022. doi:10.1007/s40620-021-01062-6.
74. **Zheleznova NN**, **Wilson PD**, **Staruschenko A.** Epidermal growth factor-mediated proliferation and sodium transport in normal and PKD epithelial cells. *Biochim Biophys Acta* 1812: 1301–1313, 2011. doi:10.1016/j.bbadis.2010.10.004.
75. **Teitelbaum I**, **Strasheim A**, **Berl T.** Epidermal growth factor-stimulated phosphoinositide hydrolysis in cultured rat inner medullary collecting tubule cells. Regulation by G protein, calcium, and protein kinase C. *J Clin Invest* 85: 1044–1050, 1990. doi:10.1172/JCI114534.
76. **Chabardes D**, **Firsov D**, **Aarab L**, **Clabecq A**, **Bellanger AC**, **Siaume-Perez S**, **Elalouf JM.** Localization of mRNAs encoding Ca2 + -inhibitable adenylyl cyclases along the renal tubule. Functional consequences for regulation of the cAMP content. *J Biol Chem* 271: 19264–19271, 1996. doi:10.1074/jbc.271.32.19264.
77. **Chien CL**, **Wu YS**, **Lai HL**, **Chen YH**, **Jiang ST**, **Shih CM**, **Lin SS**, **Chang C**, **Chern Y.** Impaired water reabsorption in mice deficient in the type VI adenylyl cyclase (AC6). *FEBS Lett* 584: 2883–2890, 2010. doi:10.1016/j.febslet.2010.05.004.
78. **Hoffert JD**, **Chou CL**, **Fenton RA**, **Knepper MA.** Calmodulin is required for vasopressin-stimulated increase in cyclic AMP production in inner medullary collecting duct. *J Biol Chem* 280: 13624–13630, 2005. doi:10.1074/jbc.M500040200.
79. **Roos KP**, **Strait KA**, **Raphael KL**, **Blount MA**, **Kohan DE.** Collecting duct-specific knockout of adenylyl cyclase type VI causes a urinary concentration defect in mice. *Am J Physiol Renal Physiol* 302: F78–F84, 2012. doi:10.1152/ajprenal.00397.2011.

AUTHOR QUERIES

AUTHOR PLEASE ANSWER ALL QUERIES 1

AQau— Please confirm the given-names and surnames are identified properly by the colors. Names will appear in PubMed exactly as shown on the approved proofs.
■ = Given-Name, ■ = Surname.

AQaff— Please confirm the Institutions and country names are identified properly by the colors given within the affiliation section.
■ = Institution, ■ = Country name.

AQ1:— Please read entire proof, answer queries, and mark corrections. Submit proof within 2 business days to the online proof review site. IMPORTANT: Please only make changes that are essential to correct data errors. Requests for nonessential changes to figures and text will not be accommodated.

AQ2:— Please check all figures, tables, equations, and legends carefully. Changes will be made only to correct scientifically relevant errors. Please confirm or correct abbreviation definitions that have been inserted in the legends by the copy editor. If changes are required to the figures themselves, please list ALL changes requested (even if you provide a new figure).

AQ3:— Please note that your manuscript has been copyedited and that style changes have been made, including those related to punctuation, abbreviations, italics, hyphens and word divisions, units of measurement, etc., to conform to Journal style preferences. Please check that no errors in meaning were inadvertently introduced. IMPORTANT: Not all of the changes are pointed out in the Author Queries, so check ALL text carefully.

AQ4:— Please carefully review the hierarchy of headings throughout your article.

AQ5:— Please check any ORCID links and/or URLs in your manuscripts to ensure they link to the intended materials.

AQ6:— Please check the affiliation details for accuracy and revise, if needed.

AQ7:— Please verify accuracy of your e-mail for correspondence.

AQ8:— Please define "RAF," "MEK," "PDZ," "RAC," "FERM," and "dDAVP" at their respective first instances in the text unless these are standard abbreviations in your field.

AQ9:— We note that gene and protein nomenclature is used in this manuscript. If appropriate, please define at first use and ensure that genes are italicized and proteins are not. Also verify if capitalization is correct for genes/proteins. Mark EVERY instance where a change is needed.

AQ10:— Was BCA written out correctly as bicinchoninic acid?

AQ11:— Note that the sentence "To identify Gene Ontology terms that are overpresented. . ." seems incomplete as given. Please revise as needed.

AQ12:— Please note that Tables 2A, 2B, and 2C have been renumbered as Tables 3, 4, and 5, and subsequent tables have been renumbered accordingly per journal style. Are the changes made okay?

AUTHOR QUERIES

AUTHOR PLEASE ANSWER ALL QUERIES 2

AQ13:— Was IP3 written out correctly as inositol (1,4,5)-trisphosphate?

AQ14:— Please note that the authors mentioned ("Breyer et al.") do not match against the reference number 12 cited in the sentence "Breyer et al. reported that EGF at 0.01 μM. . ." Please revise as needed.

AQ15:— APS now requires authors to explain their data sharing plan. Do the authors agree that "Data will be made available upon reasonable request" or should another statement be inserted in this section?

AQ16:— Please verify that the supplemental DOI link is public and active and accesses the intended supplemental material.

AQ17:— Please verify that any GRANTS are listed correctly.

AQ18:— The text in the DISCLOSURES section reflects your data entry into the Peer Review submission. Is this still complete, relevant, and accurate?

AQ19:— The text in the AUTHOR CONTRIBUTIONS section reflects your data entry into the Peer Review submission. Is this still complete and accurate? If changes are needed, please follow this template.

AQ20:— "Three paired of EGF- and vehicle-treated samples" has been changed to "three pairs of EGF- and vehicle-treated samples" in Figure 3 legend; was your meaning retained?

AQ21:— Please define "TF" and "mTOR" in Figure 7 legend

AQ22:— Please define "mTOR" in Figure 8.

AQ23:— Was HIF written out correctly as hypoxia-inducible factor?

AQ24:— Please define "mTOR" in Table 2.

AQ25:— Please define "NA" in Table 5.